Izukawa, T., Nakajima, M., Fujiwara, R., Yamanaka, H., Fukami, T., Takamiya, M., Aoki, Y., Ikushiro, S., Sakaki, T., Yokoi, T., 2009. Quantitative analysis of UDP-glucuronosyltransferase (UGT) 1A and UGT2B expression levels in human livers. Drug Metabolism and Disposition: The Biological Fate of Chemicals 37, 1759–1768.

Jia, D.M., Tabaru, A., Akiyama, T., Abe, S., Otsuki, M., 2000. Troglitazone prevents fatty changes of the liver in obese diabetic rats. Journal of Gastroenterology and Hepatology 15, 1183–1191.

Kassahun, K., Pearson, P.G., Tang, W., McIntosh, I., Leung, K., Elmore, C., Dean, D., Wang, R., Doss, G., Baillie, T.A., 2001. Studies on the metabolism of troglitazone to reactive intermediates in vitro and in vivo. Evidence for novel biotransformation pathways involving quinone methide formation and thiazolidinedione ring scission. Chemical Research in Toxicology 14, 62–70.

Katoh, M., Matsui, T., Nakajima, M., Tateno, C., Kataoka, M., Soeno, Y., Horie, T., Iwasaki, K., Yoshizato, K., Yokoi, T., 2004. Expression of human cytochromes P450 in chimeric mice with humanized liver. Drug Metabolism and Disposition: The Biological Fate of Chemicals 32, 1402–1410.

Katoh, M., Matsui, T., Okumura, H., Nakajima, M., Nishimura, M., Naito, S., Tateno, C., Yoshizato, K., Yokoi, T., 2005. Expression of human phase II enzymes in chimeric mice with humanized liver. Drug Metabolism and Disposition: The Biological Fate of Chemicals 33, 1333–1340.

Katoh, M., Sawada, T., Soeno, Y., Nakajima, M., Tateno, C., Yoshizato, K., Yokoi, T., 2007. In vivo drug metabolism model for human cytochrome P450 enzyme using chimeric mice with humanized liver. Journal of Pharmaceutical Sciences 96, 428–437.

Kinloch, R.D., Lee, C.M., van Rooijen, N., Morgan, E.T., 2011. Selective role for tumor necrosis factor-α, but not interleukin-1 or Kupffer cells, in down-regulation of CYP3A11 and CYP3A25 in livers of mice infected with a noninvasive intestinal pathogen. Biochemical Pharmacology 82, 312–321.

Nishimura, M., Yoshitsugu, H., Yokoi, T., Tateno, C., Kataoka, M., Horie, T., Yoshizato, K., Naito, S., 2005. Evaluation of mRNA expression of human drug-metabolizing enzymes and transporters in chimeric mouse with humanized liver. Xenobiotica 35, 877–890.

Ong, M.M., Latchoumycandane, C., Boelsterli, U.A., 2007. Troglitazone-induced hepatic necrosis in an animal model of silent genetic mitochondrial abnormalities. Toxicological Sciences 97, 205–213.

Saha, S., New, L.S., Ho, H.K., Chui, W.K., Chan, E.C.Y., 2010. Direct toxicity effects of sulfo-conjugated troglitazone on human hepatocytes. Toxicology Letters 195, 135–141.

Sahi, J., Black, C.B., Hamilton, G.A., Zheng, X., Jolley, S., Rose, K.A., Gilbert, D., LeCluyse, E.L., Sinz, M.W., 2003. Comparative effects of thiazolidinediones on in vitro P450 enzyme induction and inhibition. Drug Metabolism and Disposition: The Biological Fate of Chemicals 31, 439–446.

Schulz-Utermoehl, T., Sarda, S., Foster, J.R., Jacobsen, M., Kenna, J.G., Morikawa, Y., Salmu, J., Gross, G., Wilson, I.D., 2012. Evaluation of the pahrmacokinetics, biotransformation, and hepatic transporter effects of troglitazone in mice with humanized livers. Xenobiotica 42, 503–517.

Tateno, C., Yoshizane, Y., Saito, N., Kataoka, M., Utoh, R., Yamasaki, C., Tachibana, A., Soeno, Y., Asahina, K., Hino, H., Asahara, T., Yokoi, T., Furukawa, T., Yoshizato, K., 2004. Near completely humanized liver in mice shows human-type metabolic responses to drugs. American Journal of Pathology 165, 901–912.

Tettey, J.N., Maggs, J.L., Rapeport, W.G., Pirmohamed, M., Park, B.K., 2001. Enzyme induction dependent bioactivation of troglitazone and troglitazone quinone in vivo. Chemical Research in Toxicology 14, 965–974.

Tietze, F., 1969. Enzymatic method for quantitative determination of nanogram amounts of total and oxidized glutathione: applications to mammalian blood and other tissues. Analytical Biochemistry 27, 502–522.

Tomlinson, E.S., Maggs, J.L., Park, B.K., Back, D.J., 1997. Dexamethasone metabolism in vitro: species differences. Journal of Steroid Biochemistry and Molecular Biology 62, 345–352.

Toyoda, Y., Miyashita, T., Endo, S., Tsuneyama, K., Fukami, T., Nakajima, M., Yokoi, T., 2011. Estradiol and progesterone modulate halothane-induced liver injury in mice. Toxicology Letters 204, 17–24.

Toyoda, Y., Endo, S., Tsuneyama, K., Miyashita, T., Yano, A., Fukami, T., Nakajima, M., Yokoi, T., 2012. Mechanism of exacerbative effect of progesterone on drug-induced liver injury. Toxicological Sciences 126, 16–27.

Usui, T., Hashizume, T., Katumata, T., Yokoi, T., Komuro, S., 2011. In vitro investigation of the glutathione transferase M1 and T1 null genotypes as risk factors for troglitazone-induced liver injury. Drug Metabolism and Disposition: The Biological Fate of Chemicals 39, 1303–1310.

Watanabe, T., Ohashi, Y., Yasuda, M., Takaoka, M., Furukawa, T., Yamoto, T., Sanbuissho, A., Manabe, S., 1999. Was it not possible to predict liver dysfunction caused by troglitazone during the nonclinical safety studies? Reevaluation of Safety 30, 537–546.

Watanabe, T., Furukawa, T., Sharyo, S., Ohashi, Y., Yasuda, M., Takaoka, M., Manabe, S., 2000. Effect of troglitazone on the liver of a Gunn rat model of genetic enzyme polymorphism. Journal of Toxicological Sciences 25, 423–431.

Watanabe, I., Tomita, A., Shimizu, M., Sugawara, M., Yasumo, H., Koishi, R., Takahashi, T., Miyoshi, K., Nakamura, K., Izumi, T., Matusshita, Y., Furukawa, H., Haruyama, H., Koga, T., 2003. A study to survey susceptible genetic factors responsible for troglitazone-associated hepatotoxicity in Japanese patients with type 2 diabetes mellitus. Clinical Pharmacology and Therapeutics 73, 435–455.

Watanabe, T., Sagisaka, H., Arakawa, S., Shibaya, Y., Watanabe, M., Igarashi, I., Tanaka, K., Totsuka, S., Takasaki, W., Manabe, S., 2003. A novel model of continuous depletion of glutathione in mice treated with L-buthionine (S, R)-sulfoximine. Journal of Toxicological Sciences 28, 455–469.

Willey, T.A., Bekos, E.J., Gaver, R.C., Duncan, G.F., Tay, L.K., Beijnen, J.H., Farmen, R.H., 1993. High-performance liquid chromatographic procedure for the quantitative determination of paclitaxel (Taxol) in human plasma. Journal of Chromatography 621, 231–238.

Yamamoto, Y., Yamazaki, H., Ikeda, T., Watanabe, T., Iwabuchi, H., Nakajima, M., Yokoi, T., 2002. Formation of a novel quinone epoxide metabolite of troglitazone with cytotoxicity to HepG2 cells. Drug Metabolism and Disposition: The Biological Fate of Chemicals 30, 155–160.

Yamazaki, H., Shibata, A., Suzuki, M., Nakajima, M., Shimada, N., Guengerich, F.P., Yokoi, T., 1999. Oxidation of troglitazone to a quinone-type metabolite catalyzed by cytochrome P-450 2C8 and P-450 3A4 in human liver microsomes. Drug Metabolism and Disposition: The Biological Fate of Chemicals 27, 1260–1266.

Yang, J., Hao, C., Yang, D., Shi, D., Song, X., Luan, X., Hu, G., Yan, G., 2010. Pregnane X receptor is required for interleukin-6-mediated down-regulation of cytochrome P450 3A4 in human hepatocytes. Toxicology Letters 197, 219–226.

Yoshigae, Y., Konno, K., Takasaki, W., Ikeda, T., 2000. Characterization of UDP-glucuronosyltransferases (UGTs) involved in the metabolism of troglitazone in rats and humans. Journal of Toxicological Sciences 25, 433–441.

Yoshikawa, Y., Morita, M., Hosomi, H., Tsuneyama, K., Fukami, T., Nakajima, M., Yokoi, T., 2009. Knockdown of superoxide dismutase 2 enhances acetaminophen-induced hepatotoxicity in rat. Toxicology 264, 89–95.

TOXICOLOGICAL SCIENCES 130(1), 4–16 (2012)
doi:10.1093/toxsci/kfs222
Advance Access publication July 12, 2012

Metabolic Activation and Inflammation Reactions Involved in Carbamazepine-Induced Liver Injury

Satonori Higuchi,* Azusa Yano,* Shohei Takai,* Koichi Tsuneyama,† Tatsuki Fukami,* Miki Nakajima,* and Tsuyoshi Yokoi*,[1]

*Drug Metabolism and Toxicology, Faculty of Pharmaceutical Sciences, Kanazawa University, Kanazawa 920–1192, Japan; and †Department of Diagnostic Pathology, Graduate School of Medicine and Pharmaceutical Science for Research, University of Toyama, Toyama 930-0194, Japan

[1]To whom correspondence should be addressed. Fax: +81-76-234-4407. E-mail: tyokoi@p.kanazawa-u.ac.jp.

Received May 17, 2012; accepted July 3, 2012

Drug-induced liver injury is a major safety concern in drug development and clinical pharmacotherapy; however, advances in the understanding of the mechanisms of drug-induced liver injury are hampered by the lack of animal models. Carbamazepine (CBZ) is a widely used antiepileptic agent. Although the drug is generally well tolerated, only a small number of patients prescribed CBZ develop severe hepatitis. In the present study, we developed a mouse model of CBZ-induced liver injury and elucidated the mechanisms accounting for the hepatotoxicity of CBZ. Male BALB/c mice were orally administered CBZ for 5 days. The plasma levels of alanine aminotransferase and aspartate aminotransferase were prominently increased, and severe liver damage was observed via histological evaluation. The analysis of the plasma concentration of CBZ and its metabolites demonstrated that 3-hydroxy CBZ may be relevant in CBZ-induced liver injury. The hepatic glutathione levels were significantly decreased, and oxidative stress markers were significantly altered. Mechanistic investigations found that hepatic mRNA levels of toll-like receptor 4, receptor for advanced glycation end products, and their ligands were significantly increased. Moreover, the plasma concentrations of proinflammatory cytokines were also increased. Prostaglandin E_1 administration ameliorated the hepatic injury caused by CBZ. In conclusion, metabolic activation followed by the stimulation of immune responses was demonstrated to be involved in CBZ-induced liver injury in mice.

Key Words: **carbamazepine; IL-17; hepatotoxicity; metabolism; mouse model.**

Adverse drug reactions are a clinical concern and cause attrition in drug development, with hepatotoxicity being a major contributor. It is thought that many idiosyncratic drug reactions result from the production of reactive metabolites by cytochrome P450 (CYP) enzyme systems. The reactive metabolites may lead to hepatic injuries either by direct or by immune-related mechanisms (Park *et al.*, 2000).

Carbamazepine (CBZ) is a widely used antiepileptic agent. Although the drug is generally well tolerated, only a limited number of patients prescribed CBZ develop severe, potentially life-threatening idiosyncratic reactions such as agranulocytosis, hepatitis, and Stevens-Johnson syndrome (Björnsson and Olsson, 2005; Kaufman and Shapiro, 2000; Pallock, 1987). The reasons why only few individuals are affected are poorly understood. Serious CBZ-associated hepatotoxicity assumes the following two forms: (1) a hypersensitive reaction in the form of granulomatous hepatitis that presents with fever and abnormal liver functions and (2) an acute hepatitis and hepatocellular necrosis with fever and inflammation (Björnsson, 2008; Björnsson and Olsson, 2005). In addition, the presence of a specific autoantibody directed against a human liver microsomal protein in a patient who had severe hepatotoxicity with CBZ has been reported (Pirmohamed *et al.*, 1992a). Based on these reports, the liver injury associated with CBZ is thought to have an immunoallergic basis. In contrast, another antiepileptic drug, oxcarbazepine (OXC), is not likely to be associated with idiosyncratic hepatotoxicity in humans, and there have been only a few case reports showing mild or transitory liver injury (Ahmed and Siddiqi, 2006; Björnsson, 2008).

CBZ is extensively metabolized in humans to over 30 metabolites, and the most important pathway involves the formation of the stable CBZ-10,11-epoxide followed by hydroxylation to CBZ-10,11-*trans*-dihydroxy (diOH) (Lertratanangkoon and Horning, 1982; Lu and Uetrecht, 2008). Chemically reactive metabolites are also generated as shown in Figure 1. Numerous studies have assayed CBZ-induced cytotoxicity by reactive metabolites *in vitro*, and they have suggested that CBZ 2,3-epoxide and 3-hydroxy (OH) CBZ might play a role in CBZ-induced idiosyncratic drug reactions via covalent binding to the protein or the production of reactive oxygen species (ROS) (Lu and Uetrecht, 2008; Pirmohamed *et al.*, 1992b), and glutathione (GSH) and microsomal epoxide hydrolase are involved in detoxification (Pirmohamed *et al.*, 1992b). However, there are no reports of CBZ-induced hepatotoxicity in an *in vivo* animal model.

It is well known that ROS is involved in drug-induced liver injury via mitochondrial dysfunction or hepatocyte necrosis (Jaeschke *et al.*, 2002), and it was recently reported that ROS increased the expression of the toll-like receptor (TLR) and the

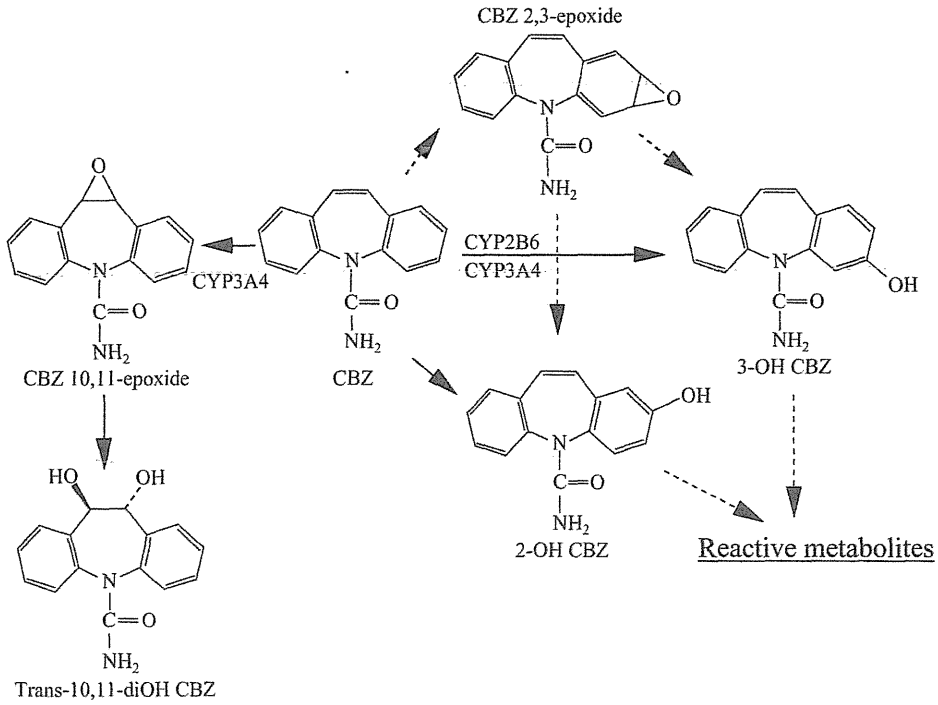

FIG. 1. The metabolic pathways of CBZ.

receptor for advanced glycation end products (RAGE), as well as their ligands, such as S100 protein and high-mobility group box 1 (HMGB1) (Yao and Brownlee, 2010). The activation of TLR or RAGE results in the induction of inflammatory cytokines and chemokines (Lotze *et al.*, 2007). Cytokines and chemokines, followed by inflammation or the infiltration of lymphocytes to hepatocytes, are involved in immune-mediated hepatotoxicity, and they are predominantly secreted from immune cells such as T lymphocytes and macrophages (Kita *et al.*, 2001; Oo and Adams, 2009). Cytokines are generated by several transcriptional factors: T-box expressed in T cells (T-bet) induces the secretion of interferon (IFN)-γ and interleukin (IL)–12; GATA-binding domain-3 (GATA-3) induces IL-4, IL-5, and IL-13 production; and retinoid-related orphan receptor (ROR)-γt promotes the production of IL-6 and IL-23, which leads to an increase in IL-17 generation (Kidd, 2003; Langrish *et al.*, 2005; Steinman, 2007).

IL-17, a T helper (Th) 17-type cytokine, acts as a potent inflammatory cytokine, and it is detected in sera and target tissues of patients with various immune-related diseases, including rheumatoid arthritis, multiple sclerosis, systemic lupus erythematosus, and asthma (Kidd, 2003; Steinman, 2007). Consistent with those observations, it has been suggested that IL-17 is involved in the pathogenesis of immune-mediated hepatotoxicities in mice, such as halothane- or α-naphthylisothiocyanate-induced hepatotoxicity (Kobayashi *et al.*, 2009, 2010).

At present, the widely studied model of drug-induced liver injury is the acetaminophen (APAP)-induced liver injury model, which commonly involves mice as the model organism. Although important information on the mechanisms of drug-induced acute inflammatory injury has been generated from this model, APAP hepatotoxicity does not encompass all possible mechanistic features of drug-induced liver injury. Therefore, it is critical to establish several animal models of drug-induced liver injury. This work is the first study to establish a mouse model of CBZ-induced hepatotoxicity. Our data suggest that metabolic activation and inflammation reactions are involved in CBZ-induced liver injury, and this is an appropriate animal model for the study of the severe hepatotoxicity induced by CBZ.

MATERIALS AND METHODS

Materials. CBZ was purchased from Wako Pure Chemical Industries (Osaka, Japan). OXC was from LKT Laboratories (St Paul, Minnesota), and 2-OH CBZ and 3-OH CBZ were from Toronto Research Chemicals (Toronto, Canada). CBZ-10, 11-epoxide and trans-10, 11-diOH CBZ were kindly provided by Novartis Pharma Inc. (Basel, Switzerland). RNAiso was from Nippon Gene (Tokyo, Japan). Fuji DRI-CHEM slides of GPT/ALT-PIII and GOT/AST-PIII used to measure alanine aminotransferase (ALT) and aspartate aminotransferase (AST), respectively, were purchased from Fujifilm (Tokyo, Japan). ReverTra Ace was from Toyobo (Tokyo, Japan). Random hexamers and SYBR Premix Ex Taq were from Takara (Osaka, Japan). All primers were commercially synthesized at Hokkaido System Sciences (Sapporo, Japan). Eritoran was kindly provided by Eisai Co. (Tokyo, Japan). Prostaglandin E_1 (PGE_1) was purchased from Nippon Chemiphar (Tokyo, Japan). The monoclonal anti-mouse IL-17 antibody, monoclonal anti-mouse/rat RAGE antibody, and monoclonal rat IgG2a isotype, used as a control, were from R&D Systems (Abingdon, UK). The rabbit polyclonal antibody against myeloperoxidase (MPO) was from DAKO (Carpinteria, CA). The Ready-SET-GO! Mouse IL-17 ELISA kit and the Mouse IL-23 ELISA kit were from eBioscience (San Diego, CA). The HMGB1 ELISA kit II was from Sino-Test Corporation (Tokyo, Japan). Other chemicals were of analytical or the highest grade commercially available.

CBZ and OXC administration. Male BALB/cCrSlc mice (8–10 weeks old, 22–27 g) were obtained from SLC Japan (Hamamatsu, Japan). Mice were housed in a controlled environment (temperature 23 ± 1°C, humidity 50 ± 10%, and 12-h light/12-h dark cycle) in the institution's animal facility with *ad libitum* access to food and water. Animals were acclimatized before use in the experiments. Mice were orally administered CBZ (in corn oil) at a dose of 400 mg/kg for 4 days and 400 to 800 mg/kg on the 5th day. As a control, mice were administered OXC at a dose of 400 mg/kg for 4 days and 800 mg/kg on the 5th day. This dosing regimen is termed "method A" in the following studies. At 1.5, 3, 6, 12, 24, 48, and 72 h after the last administration, the blood and the liver were collected. During a repeated administration study, body weight was recorded. In the single administration study, mice were administered 400 mg/kg or 800 mg/kg CBZ and were sacrificed at 3 h (for assay of the plasma concentration of CBZ and its metabolites) or 24 h (for measurement of the ALT level) after administration. A portion of each excised liver was fixed in 10% formalin neutral buffer solution and used for immunohistochemical staining. The degree of liver injury was assessed by hematoxylin and eosin (H&E) staining, and ALT and AST levels were measured by a DRI-CHEM (Fujifilm). Animal maintenance and treatment were conducted in accordance with the National Institutes of Health Guide for Animal Welfare of Japan, and the protocols were approved by the Institutional Animal Care and Use Committee of Kanazawa University, Japan.

Treatment with Cyp3a inhibitors. One hour before the last CBZ administration, ketoconazole (KTZ; 50 mg/kg in corn oil) or troleandomycin (TAO; 100 mg/kg in corn oil) was injected ip into the mice. The doses of the inhibitors have been used in previous studies (Jin *et al.*, 2009; Pellinen *et al.*, 1994). Blood samples were collected 3 h (for assay of the plasma concentration of CBZ and its metabolites) or 24 h (for measurement of the ALT and AST levels) after the last CBZ administration.

Administration of a TLR4 antagonist and an anti-mouse RAGE antibody. Mice were iv treated with eritoran, a TLR4 antagonist, (50 μg/mouse in 0.2 ml sterile saline) or ip treated with an anti-mouse RAGE antibody (100 μg anti-mouse RAGE antibody in 0.5 ml sterile PBS) 6 h after the last CBZ administration using previously described methods (Chavakis *et al.*, 2003; Savov *et al.*, 2005).

Administration of an anti-mouse IL-17 antibody. According to our previous report (Kobayashi *et al.*, 2009), in the neutralization study, mice were ip treated with anti-mouse IL-17 antibody (100 μg anti-mouse IL-17 antibody in 0.5 ml sterile PBS) 6 h after the last CBZ administration. As a control, rat IgG2a was administered (100 μg rat IgG2a in 0.5 ml sterile PBS).

Quantitation of hepatic MPO-positive cells. The infiltration of mononuclear cells was assessed by immunostaining for MPO. A rabbit polyclonal antibody against MPO was used for immunohistochemical staining of the liver as previously described (Kumada *et al.*, 2004). Five visual fields of 400× magnification (0.1 mm^2 each) were randomly selected from each MPO-immunostained specimen, and a picture was taken with a digital camera (D-33E, OLYMPUS, Tokyo). The average number of MPO-positive mononuclear cells from five randomly selected visual fields was compared among the specimens.

Treatment with PGE1. Nine hours after the last CBZ administration, mice were ip treated with PGE_1 (50 μg/mouse, dissolved in 0.5 ml sterile saline). As a control, the vehicle was administered.

Statistical analysis. The data are shown as the means ± SEM. Statistical analyses between multiple groups were performed using one-way ANOVA with Dunnett's *post hoc* test for significance between individual groups. Comparisons between two groups were carried out using two-tailed Student's *t*-tests. A value of $p < 0.05$ was considered statistically significant.

RESULTS

Evaluation of CBZ-Induced Liver Injury in BALB/c Mice

CBZ is known to cause hepatotoxicity with inflammation in only a small number of patients. To provide an experimental platform for mechanistic studies of hepatotoxicity, we sought to develop an animal model of CBZ-induced liver injury in mice. Male BALB/c mice were orally administered CBZ at a dose of 400 mg/kg for 5 days. The plasma ALT and AST levels were unaffected by CBZ administration (Fig. 2A). Next, mice were orally administered CBZ at a dose of 800 mg/kg for 5 days, resulting in severe hepatotoxicity in various mice and death in others, presumably due to pharmacological adverse effects during the repeated administration (data not shown). We then successfully established a dosing regimen for hepatic injury without fatality, named "method A," consisting of oral administrations at a dose of 400 mg/kg for 4 days and 800 mg/kg on the 5th day. Mice were administered CBZ by method A, and the plasma ALT and AST levels were significantly increased 24 and 48 h after the last CBZ administration (Fig. 2A). These effects were observed in approximately 75% of the mice. In contrast, 25% of the mice showed no hepatotoxicity, and thus, the SEM values were large. The plasma ALT levels were higher than the AST levels, suggesting that tissue damage induced by CBZ administration might occur predominantly in liver. OXC, which was used as negative control, did not induce hepatotoxicity in the same dosing conditions. During the repeated administration study, the body weight of the mice did not change (data not shown).

We altered the dose of CBZ on the 5th day to 400, 600, or 800 mg/kg. No change in the plasma ALT level was observed in mice administered 400 or 600 mg/kg, whereas the dose of 800 mg/kg induced severe liver injury (Fig. 2B). In the single administration study, the plasma ALT level did not change after any of the experimental doses (Fig. 2C).

In the histological evaluation study, focal necrosis and loss of hepatocytes around the central vein were observed 24 h after the last CBZ administration with method A (Fig. 2D). No histopathological differences were observed among no treatment (NT), the lower dose of CBZ-administered (400 mg/kg for 5 days) and OXC-administered mice (Fig. 2D).

Analysis of the Plasma Concentration of CBZ and Its Metabolites

Changes in the plasma concentration of CBZ and its metabolites, CBZ-10,11-epoxide, trans-10,11-diOH CBZ, 2-OH CBZ, and 3-OH CBZ, were measured in mice with CBZ-induced liver injury. The maximum plasma concentrations of CBZ, CBZ-10,11-epoxide, and trans-10,11-diOH CBZ were observed 1.5 h after the last CBZ administration. In contrast, the time of the highest concentration of 3-OH CBZ was 3 h postadministration (Fig. 3A). The plasma concentration of 2-OH CBZ was too low to detect (data not shown). After the peak times, the plasma concentrations of CBZ and the three metabolites decreased dependently of time (Fig. 3A).

Effects of Cyp3a Inhibitors on CBZ-Induced Liver Injury

CBZ induces many drug metabolism enzymes including CYP3A and CYP2B in the liver (Oscarson *et al.*, 2006).

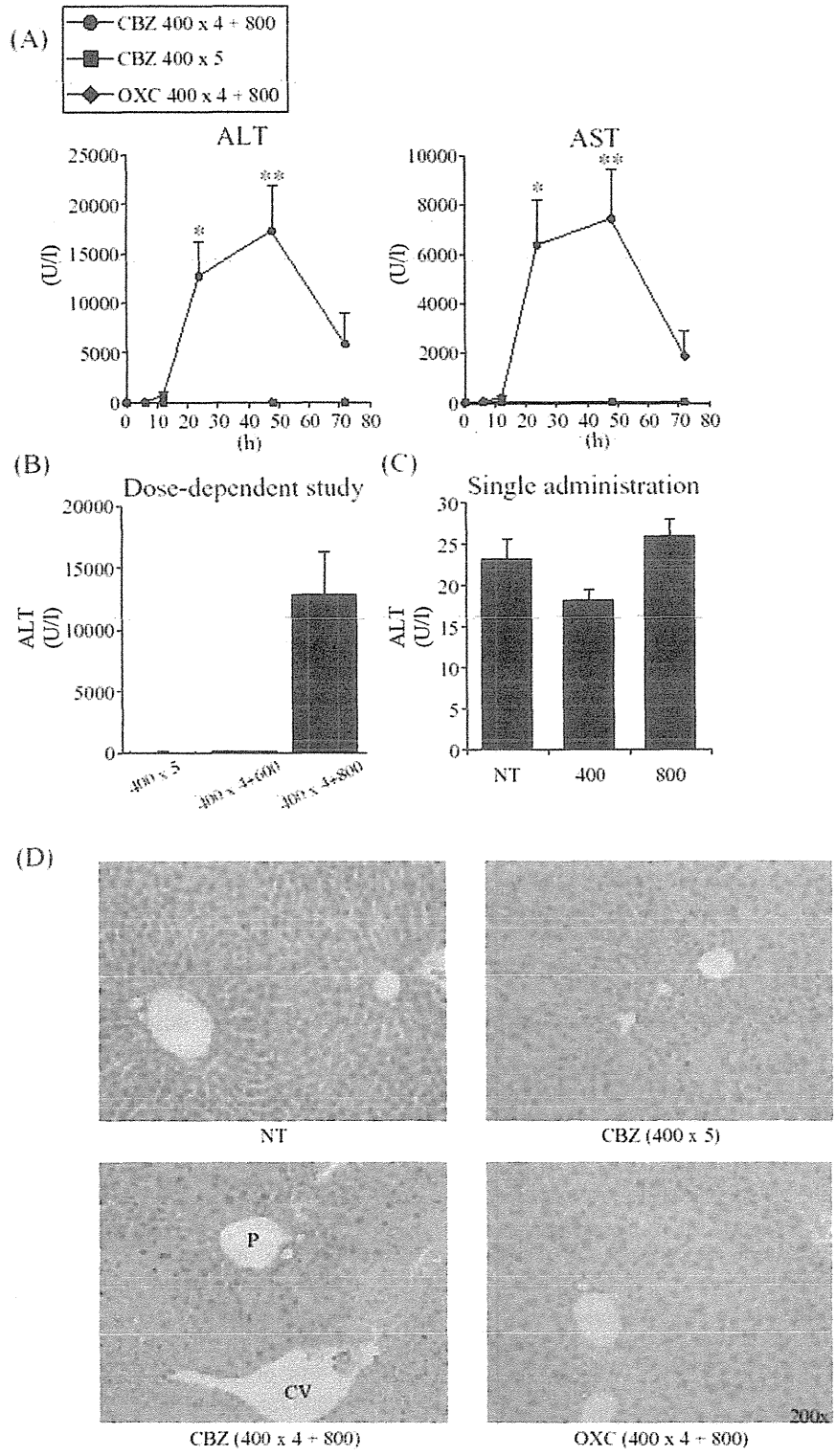

FIG. 2. Time- and dose-dependent changes in plasma ALT and AST levels in CBZ-induced liver injury. Male BALB/c mice were orally administered CBZ by method A (400 mg/kg for 4 days and 800 mg/kg on the 5th day) or 400 mg/kg for 5 days. As the control, mice were administered OXC by method A. At 1.5, 3, 6, 12, 24, 48, and 72 h after the last administration, the blood was collected for assessment of the plasma ALT and AST levels (A). In a dose-dependent study, mice were administered CBZ at a dose of 400 mg/kg for 4 days and 400–800 mg/kg on the 5th day, and blood was collected for assessment of the plasma ALT level 24 h after the last administration (B). In a single administration study, mice were administered CBZ at a dose of 400 mg/kg or 800 mg/kg, and blood was collected 24 h after administration (C). Liver tissue sections were stained with H&E (D). The data are shown as the means ± SEM of the results of the method A group from eight mice and other groups from five mice. Differences compared with the control (0 h) mice were considered significant at $*p < 0.05$ and $**p < 0.01$.

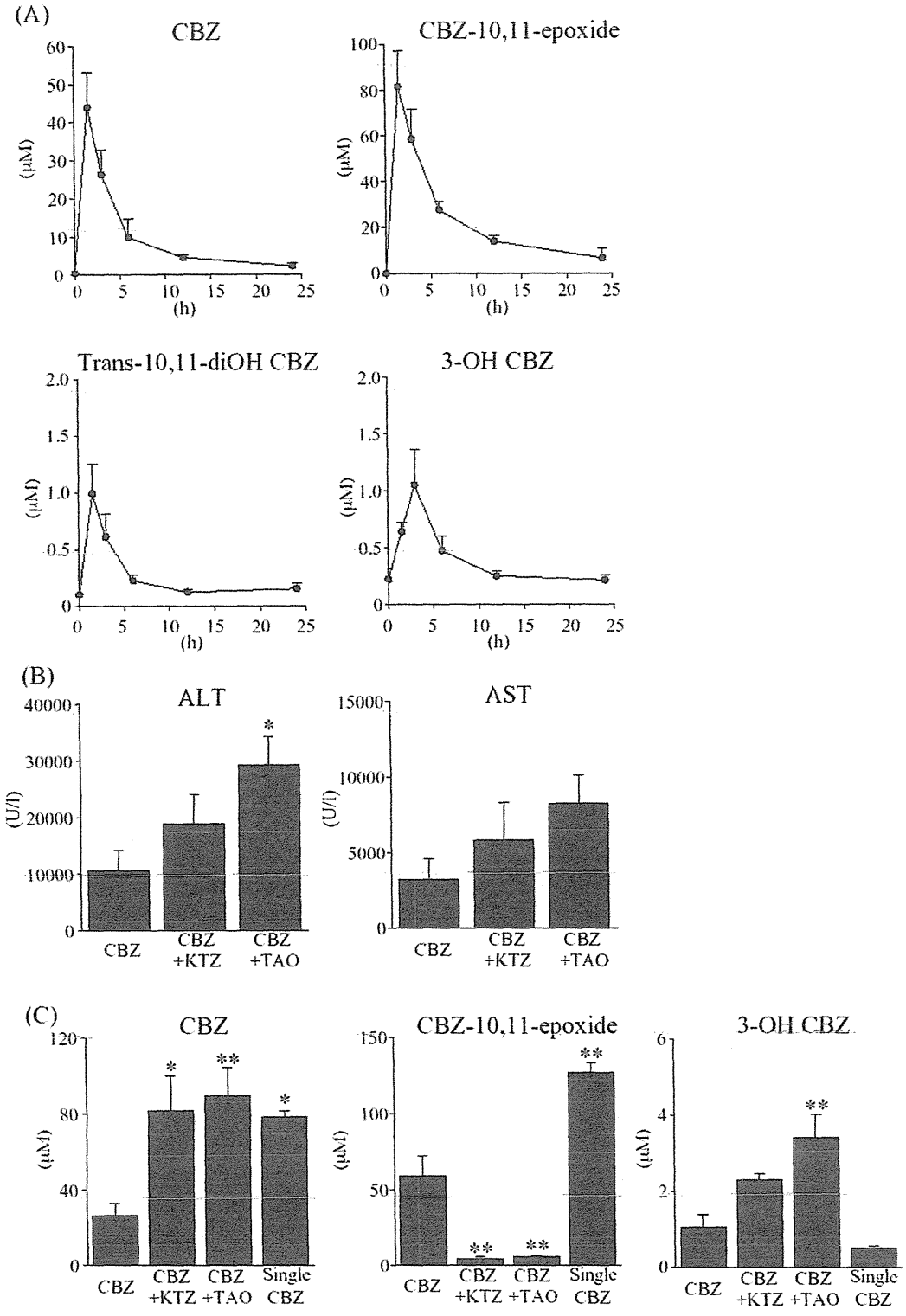

FIG. 3. Changes in the plasma concentration of CBZ and its metabolites and plasma ALT and AST levels in CBZ-induced liver injury. Mice were orally administered CBZ by method A. At 1.5, 3, 6, 12, and 24 h after the last CBZ administration, the blood was collected for assessment of CBZ and its metabolites in plasma (A). The data are shown as the means ± SEM of the results from five mice. The plasma ALT and AST levels and the concentration of CBZ and its metabolites were measured after the administration of Cyp inhibitors in mice with CBZ-induced liver injury (B and C). One hour before the last CBZ administration, KTZ (50 mg/kg in corn oil) or TAO (100 mg/kg in corn oil) was ip administered. Blood samples were collected 3 h (for assay of the plasma concentration of CBZ and its metabolites) or 24 h (for measurement of the ALT and AST levels) after the last CBZ administration. The data are shown as the means ± SEM of the results from five mice. Differences compared with the CBZ-alone-administered mice were considered significant at $*p < 0.05$ and $**p < 0.01$.

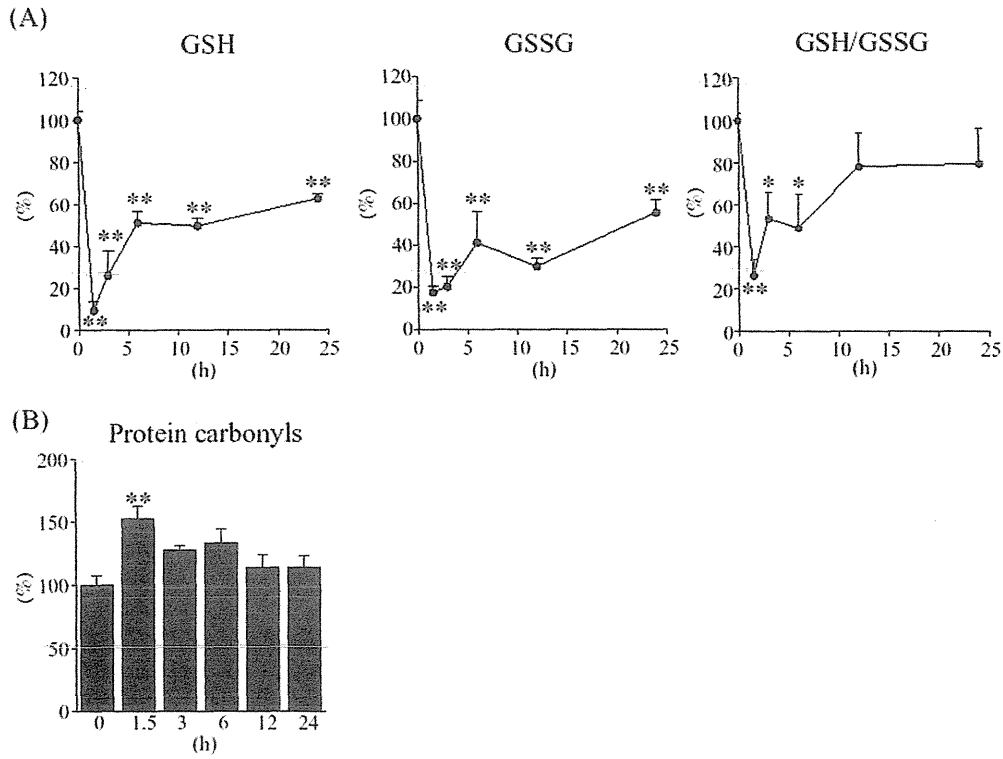

FIG. 4. Time-dependent changes in hepatic GSH, GSSG, and oxidative stress marker levels. Mice were orally administered CBZ by method A. At 1.5, 3, 6, 12, and 24 h after the last CBZ administration, the livers and the plasma were collected for assessment of the hepatic GSH and GSSG levels and GSH/GSSG ratio (A) and the content of plasma protein carbonyls (B). The data are shown as the means ± SEM of the results from five mice. Differences compared with the 0 h mice were considered significant at $*p < 0.05$ and $**p < 0.01$.

CYP3A metabolizes CBZ into CBZ-10,11-epoxide, 3-OH CBZ, and reactive metabolites *in vitro* (Lu and Uetrecht, 2008; Pirmohamed *et al.*, 1992b), leading to the hypothesis that CYP3A may be involved in CBZ-induced toxicity. To investigate whether Cyp3a is involved in CBZ-induced liver injury *in vivo*, mice were treated with the Cyp3a inhibitors KTZ or TAO. Surprisingly, the plasma ALT levels significantly increased after TAO treatment and exhibited an increasing trend after KTZ treatment in CBZ-administered mice. The plasma AST levels also exhibited an increasing trend after KTZ or TAO treatment in CBZ-administered mice (Fig. 3B). Single administration of KTZ (50 mg/kg, ip) or TAO (100 mg/kg, ip) caused no increase in the plasma ALT level 1 h (24.2±6.3 U/l or 27.3±3.7 U/l, respectively) and 25 h (19.8±6.6 U/l or 19.3±5.4 U/l, respectively) after the administration, suggesting KTZ or TAO did not induce hepatotoxicity in the present dosing condition.

The plasma concentrations of CBZ, CBZ-10,11-epoxide, and 3-OH CBZ 3 h after the coadministration of CBZ and KTZ or TAO are shown in Figure 3C. Mice that were administered a single dose of CBZ (800 mg/kg), which caused no hepatotoxicity (Fig. 2C), were used as negative controls. KTZ or TAO treatment significantly increased the plasma concentration of CBZ and significantly decreased the concentration of CBZ-10,11-epoxide, whereas the plasma concentrations of both compounds were significantly increased in mice administered a single dose of CBZ. KTZ exhibited an increasing trend and TAO significantly increased 3-OH CBZ, which exhibited a decreasing trend in mice administered a single dose of CBZ. These data suggest that Cyp3a might be involved in detoxification in CBZ-induced liver injury.

To confirm the Cyp induction by CBZ or OXC with the administration by method A, we measured Cyp3a activity in the microsomes of mice using the metabolism of midazolam as an indicator. The Cyp3a activities were significantly higher in both CBZ- and OXC-administered mice compared with NT mice (Supplementary fig. 1). Because Cyp3a activity was significantly increased in OXC-administered mice, mice were coadministered OXC and TAO, but plasma ALT or AST level was not changed (data not shown).

Changes in GSH Levels and the GSH/Glutathione Disulfide Ratio in the Liver

To investigate whether GSH is involved in detoxification *in vivo* in mice, time-dependent changes in GSH and glutathione disulfide (GSSG) levels in the liver were measured. The GSH level was the lowest 1.5 h after the last CBZ administration and was significantly decreased at 1.5, 3, 6, 12, and 24 h compared with mice at 0 h (time for the final administration of CBZ). GSSG level exhibited a similar profile (Fig. 4A).

We measured the GSH/GSSG ratio, a biomarker of oxidative stress (Fig. 4A). The ratio of GSH/GSSG was significantly

decreased 1.5, 3, and 6 h after the last CBZ administration. In addition, the level of protein carbonyls, which is also a marker of oxidative stress, was significantly increased 1.5 h after the last CBZ administration (Fig. 4B). These results suggested that GSH played a protective role, and oxidative stress is involved in an early stage of CBZ-induced liver injury.

The Expressions of Danger Signals and Their Receptors

It has been reported that ROS elevated the expression levels of danger signals, such as S100A8, S100A9, and HMGB1 (Yao and Brownlee, 2010). To investigate whether danger signals are involved in the onset of inflammation, time-dependent changes in the mRNA expression levels of S100A8, S100A9, HMGB1, TLR2, TLR4, TLR9, and RAGE were measured (Fig. 5A). The mRNA expression levels of S100A8 and S100A9 were time-dependently increased and significantly increased 24 h after the last CBZ administration. The expression of TLR4 was significantly increased at 6 h, and the expression level of RAGE was significantly increased at 12 h postadministration; however, the expression levels of HMGB1, TLR2, and TLR9 were not altered. In OXC-administered mice, the mRNA expression levels of danger signal–related genes were not changed compared with the NT control. It is known that HMGB1 is actively secreted from activated immune cells and is also passively released from necrotic cells (Wang *et al.*, 2004). Thus, the release of HMGB1 is not correlated with the increased expression of hepatic HMGB1 mRNA. The plasma concentration of HMGB1 protein was measured using ELISA, and it was significantly increased at 24 h (Fig. 5B).

To investigate whether TLR4 and RAGE signaling were involved in CBZ-induced liver injury, eritoran, a TLR4 antagonist, or a monoclonal anti-RAGE antibody was administered to the mice. Eritoran or anti-RAGE antibody treatment significantly suppressed the plasma ALT and AST levels (Fig. 5C). These results suggested that TLR4 and RAGE activation might be involved in CBZ-induced liver injury.

The Involvement of Cytokines and Chemokines

To investigate the involvement of inflammatory factors in CBZ-induced liver injury, time-dependent changes in the mRNA expression levels of transcriptional factors, cytokines, and chemokines were measured (Fig. 6A). The expression level of ROR-γt was significantly increased 12 h after the last CBZ administration compared with that of NT mice. T-bet was significantly decreased, and GATA-3 was not altered. The expression levels of IL-6, IL-23 p19, FasL, and macrophage inflammatory protein-2 (MIP-2) were significantly increased compared with those of NT mice, whereas IL-12 p35 and IFN-γ were significantly decreased (Fig. 6A). The expression level of IL-17 mRNA was too low to detect (data not shown). In OXC-administered mice, the mRNA expression levels of cytokines and chemokines were not changed compared with the levels in the NT controls.

The plasma concentrations of IL-17 and IL-23 protein measured by ELISA were significantly increased 24 h after the last CBZ administration (Fig. 6B). The plasma concentration of IFN-γ protein could not be detected at any of the tested time points (data not shown).

To investigate whether IL-17 was involved in CBZ-induced liver injury, we conducted a neutralization study. A monoclonal anti-mouse IL-17 antibody was ip administered 9 h after the last CBZ administration, resulting in significantly reduced plasma ALT and AST levels 24 h after the last CBZ administration (Fig. 6C). These effects were not observed after the administration of an IgG control antibody. In the histopathological evaluation study, anti-mouse IL-17 antibody treatment significantly decreased the number of MPO-positive cells (Fig. 6D). Representative photographs of anti-MPO staining are shown in Supplementary figure 2.

Effects of PGE_1 Treatment

PGEs are known to protect against drug-induced and immune-mediated liver injury by downregulating the production of inflammatory cytokines. PGE_1 inhibited the function of neutrophils (Talpain *et al.*, 1995) and the production of IL-17 (Kobayashi *et al.*, 2009). It was reported that IL-6 and IL-23 induced IL-17 production (Langrish *et al.*, 2005). On the basis of these studies, we hypothesized that PGE_1 might decrease the production of IL-6 and IL-23 in the present study. PGE_1 conjugated by α-cyclodextrin was ip injected into mice 9 h after the last CBZ administration according to the method reported previously (Kobayashi *et al.*, 2009). The plasma ALT and AST levels were significantly decreased by PGE_1 treatment in CBZ-administered mice compared with CBZ alone-administered mice (Fig. 7A). PGE_1 administration significantly suppressed the hepatic mRNA expression of IL-6, IL-23p19, and MIP-2 (Fig. 7B). The plasma concentrations of IL-17 and IL-23 proteins were also decreased (Fig. 7C).

DISCUSSION

Advances in the understanding of the mechanisms of drug-induced liver injury have been hampered by the lack of proper animal models. Mouse models of APAP-induced liver injury are the widespread model, but this model alone cannot encompass the entire spectrum of the clinical and mechanistic features of drug-induced liver injury in patients. In the present study, we developed a mouse model of CBZ-induced liver injury. This model provided novel mechanistic information, including aspects of drug metabolism and inflammation in the pathogenesis of CBZ-induced liver injury.

Subacute toxicity study demonstrated that no evidence of hepatotoxicity was observed after repeated administrations of CBZ (200 mg/kg, orally) once daily for 24 weeks to mice (Novartis Pharma Co., 2011). After investigating many different dosing conditions, we found that CBZ at a dose of 400 mg/kg for 4 days and 800 mg/kg on the 5th day (method A) induced prominent hepatotoxicity, but 400 mg/kg for 5 days did not (Fig. 2A). The maximum plasma concentration of CBZ

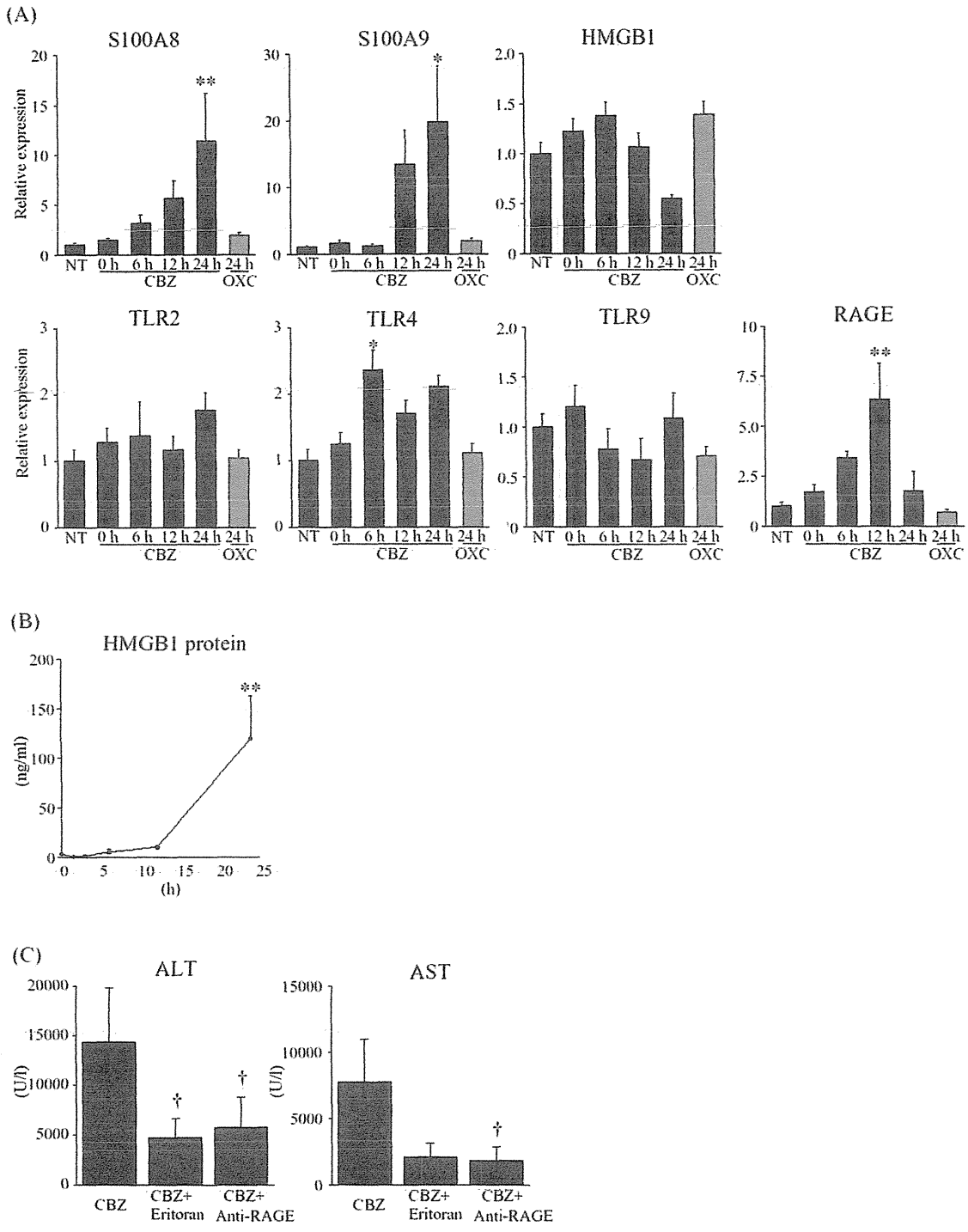

FIG. 5. Time-dependent changes in the mRNA expression levels of danger signal–related genes in the liver of CBZ-administered mice (A) and the plasma HMGB1 protein levels in CBZ-administered mice (B). Mice were orally administered CBZ by method A, and the livers and plasma were collected 0, 6, 12, and 24 h after the last CBZ administration for assessment of the expression levels of the hepatic mRNA or the plasma protein levels. As the control, mice were orally administered OXC by the same method A, and the livers and plasma were collected 24 h after the last OXC administration. The expression of hepatic mRNA was normalized to that of β-actin. The effects of the administration of eritoran, a TLR4 antagonist, or anti-RAGE-monoclonal antibody on CBZ-induced liver injury (C). Mice were iv administered eritoran (50 μg/mouse in 0.1 ml sterile saline) or ip anti-mouse RAGE antibody (100 μg anti-RAGE antibody in 0.5 ml sterile PBS) 6 h after the last CBZ administration. Blood samples were collected 24 h after the last CBZ administration. The data are shown as the means ± SEM of the results of the time-dependent study from five mice, the method A group from eight mice, and the other groups from five mice. Differences compared with the 0 h mice were considered significant at $^{*}p < 0.05$ and $^{**}p < 0.01$, and differences compared with the CBZ-alone-administered mice were considered significant at $\dagger p < 0.05$.

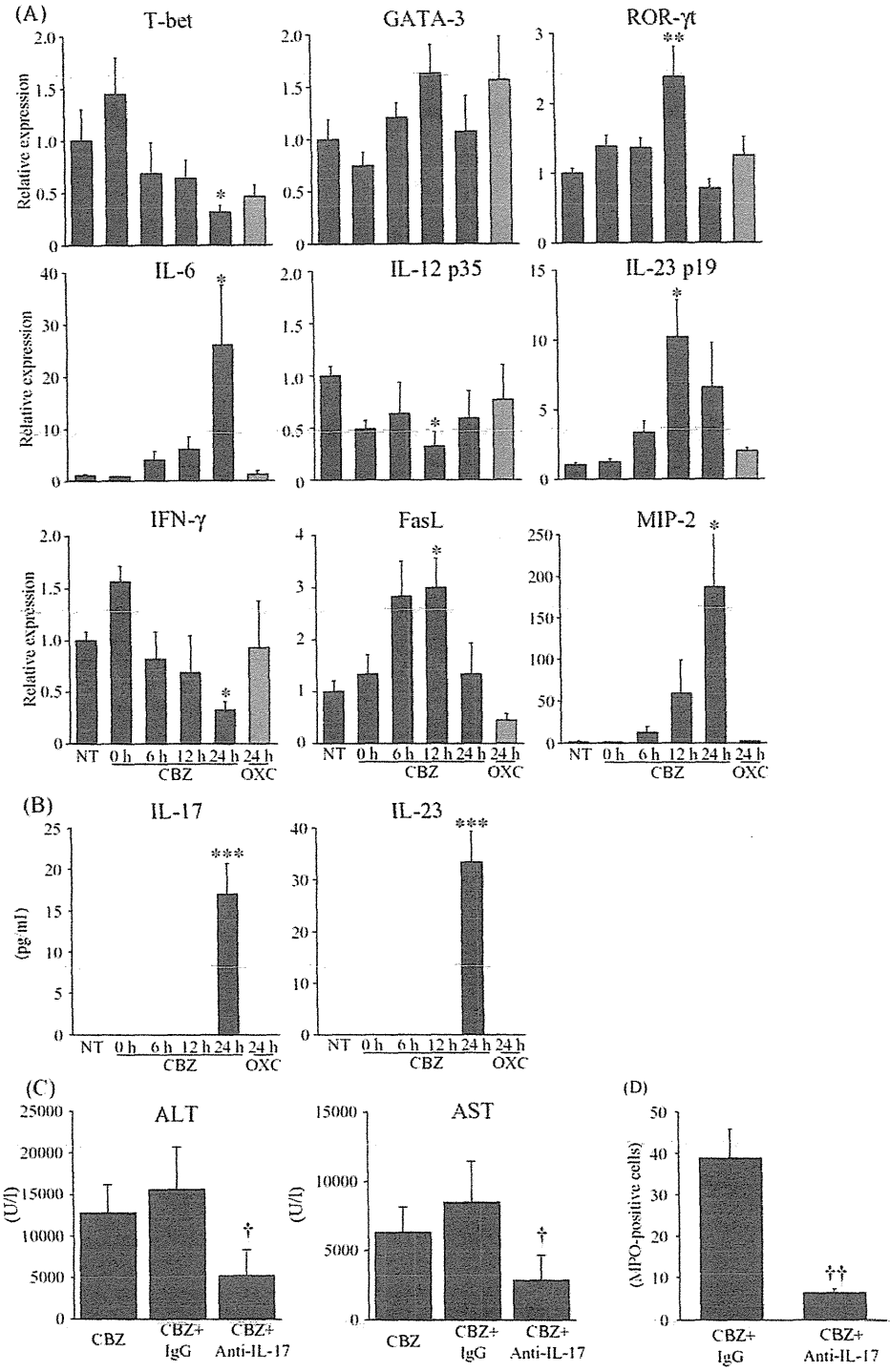

FIG. 6. Time-dependent changes in the hepatic mRNA expression levels and plasma protein levels of proinflammatory cytokines and chemokines in CBZ-induced liver injury (A and B). Mice were orally administered CBZ by method A, and the livers and the plasma were collected 0, 6, 12, and 24 h after the last CBZ administration for assessment of the expression levels of the hepatic mRNA by real-time RT-PCR or the plasma protein levels by ELISA. Mice were orally administered OXC by the same method A, and the livers and plasma were collected 24 h after the last administration. The expression of hepatic mRNA was normalized to that of β-actin. The data are shown as the means ± SEM of the results from five mice. Differences compared with the NT mice were considered significant at $*p < 0.05$, $**p < 0.01$, and $***p < 0.001$. The neutralization study of IL-17 in CBZ-induced liver injury (C). Mice were ip administered an anti-mouse IL-17 antibody (100 μg anti-mouse IL-17 antibody in 0.5 ml sterile PBS) 6 h after the last CBZ administration. As a control, rat IgG2a was administered (100 μg rat IgG2a in 0.5 ml sterile PBS). The number of MPO-positive cells in CBZ-alone-administered mice or CBZ and anti-IL-17-administered mice (D). The infiltration of mononuclear cells was assessed by immunostaining for MPO. The data are shown as the means ± SEM of the results of the method A group from eight mice and the other group from six mice. Differences compared with the CBZ- and IgG-administered mice were considered significant at $\dagger p < 0.05$ and $\dagger\dagger p < 0.01$.

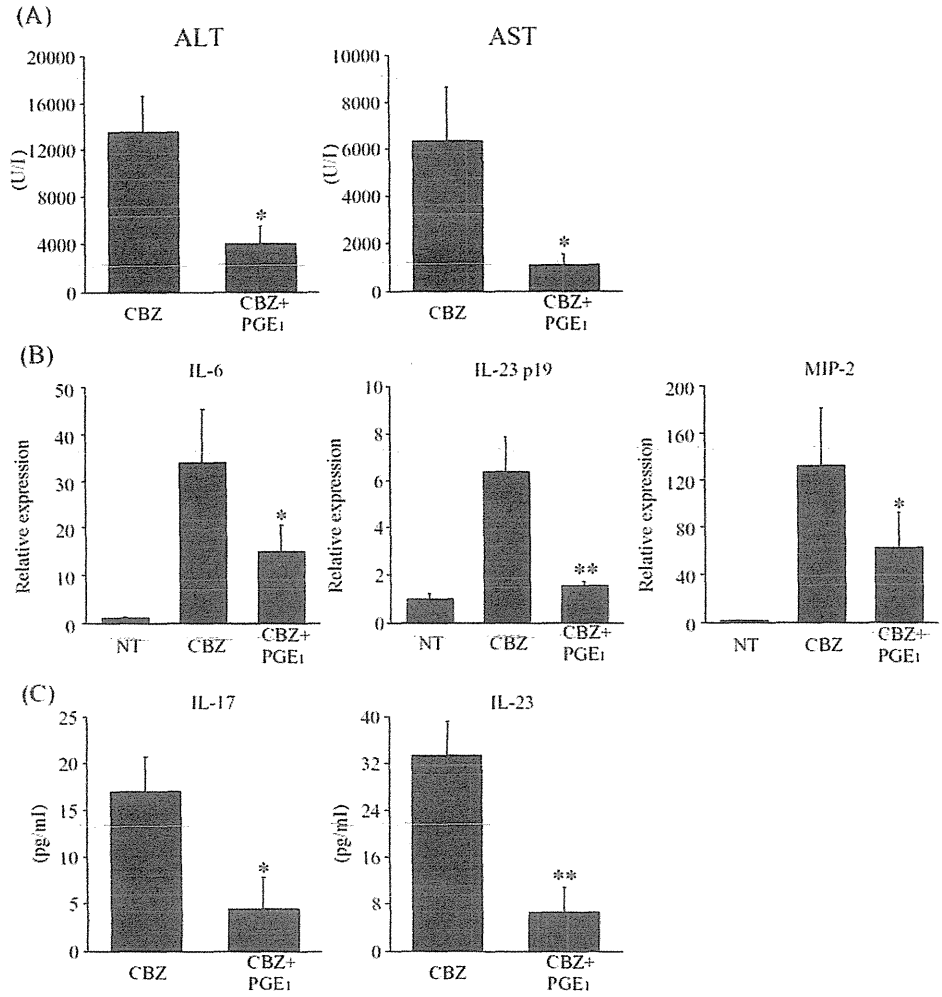

FIG. 7. The effects of PGE_1 administration on CBZ-induced liver injury. Mice were orally administered CBZ by method A, and mice were ip treated with PGE_1 (50 μg/mouse, dissolved in 0.5 ml sterile saline) 9 h after the last administration. As a control, vehicle was administered. At 24 h after the last CBZ administration, the livers and plasma were collected for the assessment of plasma ALT and AST levels (A), the expression levels of the hepatic mRNA of IL-6, IL-23 p19 and MIP-2 (B), and the plasma protein levels of IL-17 and IL-23 (C). The expression levels of hepatic mRNA were normalized to that of β-actin. The data are shown as the means ± SEM of the results of the method A group from seven mice and the CBZ and PGE_1 group from six mice. Differences compared with the CBZ-alone-administered mice were considered significant at $^*p < 0.05$ and $^{**}p < 0.01$.

1.5 h after the last administration (43.8±20.7μM) was nearly equal to the steady-state human plasma concentration of CBZ (Eichelbaum *et al.*, 1975). In clinical therapeutics, the dosage of CBZ is gradually increased for the maintenance of the therapeutic plasma concentration because CBZ is a potent inducer of microsomal drug metabolism (Oscarson *et al.*, 2006). In fact, CBZ induced the Cyp3a enzyme activity in our novel mouse model (Supplementary fig. 1). Based on our findings, it was suggested that the escalation of the dosage for the maintenance of the therapeutic plasma concentration caused the risk for CBZ-induced liver injury. In addition, the single administration of CBZ at a dose of 800 mg/kg did not induce hepatotoxicity (Fig. 2C), suggesting that repeated administration is necessary to cause CBZ-induced liver injury. Due to the presence of a specific autoantibody directed against a human liver microsomal protein in a patient who had severe hepatotoxicity with CBZ (Pirmohamed *et al.*, 1992a), the induction of drug metabolism enzymes and/or the generation of antibodies directed against CBZ-protein conjugates during repeated administration may be involved in CBZ-induced liver injury. The dosing method of CBZ in the present study might be useful for the development of animal models for other drug-induced liver injury.

In the histopathological study, remarkable hepatic necrosis and loss of hepatocytes, especially around the central vein, were observed in the mice administered CBZ by method A, and these effects were similar to APAP-induced liver injury (Antoine *et al.*, 2009). Because Cyps are mainly expressed around the central vein in the liver, this observation suggested that Cyps may be involved in CBZ-induced liver injury. CBZ-associated severe hepatotoxicity takes the following two forms: (1) a

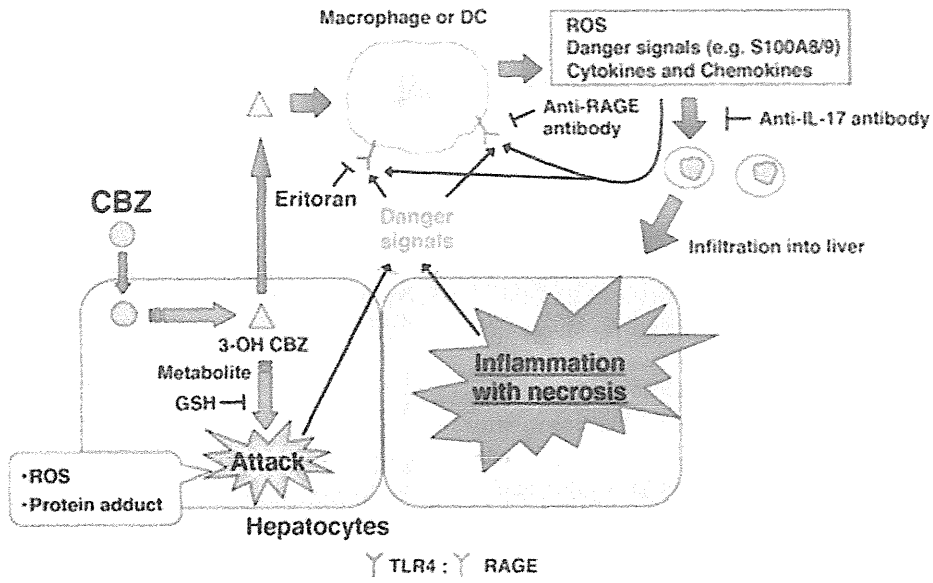

FIG. 8. A proposed mechanism of CBZ-induced liver injury. CBZ is metabolized in hepatocytes by Cyps, the produced reactive metabolite(s) induce ROS production in macrophages, and then danger signals released from macrophage activate TLR4 and RAGE. The activated TLR4 and RAGE lead to the secretion of proinflammatory cytokines and chemokines, which result in inflammation in the liver. The necrotic hepatocytes secrete the ligands of TLR4 and RAGE, which induce further inflammation in the liver.

hypersensitive reaction in the form of granulomatous hepatitis that present with fever and abnormal liver functions and (2) an acute hepatitis and hepatocellular necrosis with inflammation (Björnsson, 2008; Björnsson and Olsson, 2005). The mouse model in the present study may fit the latter form.

Changes in the plasma concentration of 3-OH CBZ suggested a certain role for the metabolite in CBZ-induced liver injury in the present study. Additionally, 2-OH CBZ, which is also a potential reactive metabolite, was not detected in plasma, which is coincident with a report that 2-OH CBZ is generated to a much lesser extent than 3-OH CBZ *in vitro* (Pearce *et al.*, 2002). Based on these results, 2-OH CBZ may not likely to be involved in CBZ-induced liver injury *in vivo*. It has been reported that 3-OH CBZ, a reactive metabolite produced by a variety of CYPs, induced ROS causing mitochondrial dysfunctions (Pearce *et al.*, 2008), which causes the suppression of GSH levels and the alteration of oxidative stress markers. CYP3A4 and CYP2B6 are largely responsible for the formation of 3-OH CBZ in humans (Pearce *et al.*, 2002), and these enzymes are induced by CBZ treatment. Therefore, repeated administration of a high dose of CBZ may cause the elevation of 3-OH CBZ. Because there is no direct evidence that 3-OH CBZ is a reactive metabolite or is related to the production of reactive metabolite(s), further studies are needed to examine these possibilities. In addition, 3-OH CBZ cannot be used directly for accessing hepatotoxicity due to different *in vivo* distribution and pharmacokinetics compared with CBZ. Treatment with Cyp3a inhibitors exacerbated the hepatic injury caused by CBZ (Fig. 3B), suggesting that the main function of Cyp3a is detoxification in CBZ-induced liver injury. Contrary to this result, Pirmohamed *et al.* (1992b) demonstrated that KTZ reduced the cytotoxicity of bioactivated CBZ by liver microsomes from phenobarbital-administered mice. The difference in the results between *in vitro* and *in vivo* systems is not unusual and should be carefully evaluated, especially in cases involving enzyme induction.

It has recently been reported that ROS induced the expression of the ligands of TLR4 and RAGE (Yao and Brownlee, 2010), and inflammation in the liver through the activation of TLR4 or RAGE is involved in APAP-induced liver injury (Antoine *et al.*, 2009). On the basis of these experimental results, we demonstrated that the activation of TLR4 and RAGE by ROS is the essential factor in relation to the drug metabolism and inflammation in CBZ-induced liver injury. Mu *et al.* (2011) demonstrated that the activation of TLR4 prompted the generation of Th17-associated cytokines. Therefore, the activation of TLR4 and RAGE might induce the generation of Th17-associated cytokines, resulting in inflammation in the liver in the present study.

IL-17 induced by IL-6 and IL-23 stimulates the production of CXC-chemokines (such as MIP-2 and keratinocyte-derived chemokine) and activates neutrophils (Langrish *et al.*, 2005; Steinman, 2007). IL-17 was involved in the pathogenesis of various autoimmune diseases and immune-mediated hepatotoxicity in mice (Kobayashi *et al.*, 2009, 2010). These lines of evidence prompted us to confirm the involvement of IL-17 in CBZ-induced liver injury. The neutralization of IL-17 reduced the plasma ALT and AST levels and MPO-positive cells in the liver (Figs. 6C and D), which suggested that infiltration of neutrophils into the liver via IL-17 was involved in CBZ-induced liver injury.

PGE_1 treatment 9 h after the last CBZ administration ameliorated CBZ-induced liver injury (Fig. 7A), and PGE_1 suppressed the production of IL-6 and IL-23, resulting in the decrease of plasma IL-17 concentration (Figs. 7B and C). PGE_1 inhibited superoxide production by neutrophils *in vitro* (Talpain *et al.*, 1995) and had a protective effect against halothane-induced liver injury by the neutralization of IL-17 in mice (Kobayashi *et al.*, 2009). Additionally, PGE_1 had protective effects on livers suffering from ischemia/reperfusion injury and decreased the plasma IL-6 levels in humans (Sugawara *et al.*, 1998). PGE_1 could be used for pharmacotherapy of CBZ-induced liver injury in clinical practice.

CBZ causes not only hepatotoxicity but also cutaneous drug reactions, including maculopapular eruption, hypersensitivity syndrome, Stevens-Johnson syndrome, and toxic epidermal necrolysis. It is well known that human leukocyte antigen alleles are strongly associated with CBZ-induced cutaneous adverse drug reactions (Hung *et al.*, 2006). In the present study, cutaneous drug reactions were not observed in the mouse model of CBZ-induced liver injury. Thus, the development of an experimental animal model of CBZ-induced cutaneous adverse drug reactions is still needed.

In conclusion, we developed a mouse model of CBZ-induced liver injury. Based on the results of the present study, the proposed mechanisms are summarized in Figure 8. Information resulting from our novel mouse model could eventually be applied to preclinical drug development.

SUPPLEMENTARY DATA

Supplementary data are available online at http://toxsci.oxfordjournals.org/.

FUNDING

Health and Labor Sciences Research Grants from the Ministry of Health, Labor and Welfare of Japan (H23-BIO-G001).

REFERENCES

Ahmed, S. N., and Siddiqi, Z. A. (2006). Antiepileptic drugs and liver disease. *Seizure* **15,** 156–164.

Antoine, D. J., Williams, D. P., Kipar, A., Jenkins, R. E., Regan, S. L., Sathish, J. G., Kitteringham, N. R., and Park, B. K. (2009). High-mobility group box-1 protein and keratin-18, circulating serum proteins informative of acetaminophen-induced necrosis and apoptosis *in vivo*. *Toxicol. Sci.* **112,** 521–531.

Björnsson, E., and Olsson, R. (2005). Outcome and prognostic markers in severe drug-induced liver disease. *Hepatology* **42,** 481–489.

Björnsson, E. (2008). Hepatotoxicity associated with antiepileptic drugs. *Acta Neurol. Scand.* **118,** 281–290.

Chavakis, T., Bierhaus, A., Al-Fakhri, N., Schneider, D., Witte, S., Linn, T., Nagashima, M., Morser, J., Arnold, B., Preissner, K. T., *et al.* (2003). The pattern recognition receptor (RAGE) is a counterreceptor for leukocyte integrins: A novel pathway for inflammatory cell recruitment. *J. Exp. Med.* **198,** 1507–1515.

Eichelbaum, M., Ekbom, K., Bertilsson, L., Ringberger, V. A., and Rane, A. (1975). Plasma kinetics of carbamazepine and its epoxide metabolite in man after single and multiple doses. *Eur. J. Clin. Pharmacol.* **8,** 337–341.

Hung, S. I., Chung, W. H., Jee, S. H., Chen, W. C., Chang, Y. T., Lee, W. R., Hu, S. L., Wu, M. T., Chen, G. S., Wong, T. W., *et al.* (2006). Genetic susceptibility to carbamazepine-induced cutaneous adverse drug reactions. *Pharmacogenet. Genomics* **16,** 297–306.

Jaeschke, H., Gores, G. J., Cederbaum, A. I., Hinson, J. A., Pessayre, D., and Lemasters, J. J. (2002). Mechanisms of hepatotoxicity. *Toxicol. Sci.* **65,** 166–176.

Jin, H., Dai, J., Chen, X., Liu, J., Zhong, D., Gu, Y., and Zheng, J. (2009). Pulmonary toxicity and metabolic activation of dauricine in CD-1 mice. *J. Pharmacol. Exp. Ther.* **332,** 738–746.

Kaufman, D. W., and Shapiro, S. (2000). Epidemiological assessment of drug-induced disease. *Lancet* **356,** 1339–1343.

Kidd, P. (2003). Th1/Th2 balance: The hypothesis, its limitations, and implications for health and disease. *Altern. Med. Rev.* **8,** 223–246.

Kita, H., Mackay, I. R., Van De Water, J., and Gershwin, M. E. (2001). The lymphoid liver: Considerations on pathways to autoimmune injury. *Gastroenterology* **120,** 1485–1501.

Kobayashi, E., Kobayashi, M., Tsuneyama, K., Fukami, T., Nakajima, M., and Yokoi, T. (2009). Halothane-induced liver injury is mediated by interleukin-17 in mice. *Toxicol. Sci.* **111,** 302–310.

Kobayashi, M., Higuchi, S., Mizuno, K., Tsuneyama, K., Fukami, T., Nakajima, M., and Yokoi, T. (2010). Interleukin-17 is involved in alpha-naphthylisothiocyanate-induced liver injury in mice. *Toxicology* **275,** 50–57.

Kumada, T., Tsuneyama, K., Hatta, H., Ishizawa, S., and Takano, Y. (2004). Improved 1-h rapid immunostaining method using intermittent microwave irradiation: Practicability based on 5 years application in Toyama Medical and Pharmaceutical University Hospital. *Mod. Pathol.* **17,** 1141–1149.

Langrish, C. L., Chen, Y., Blumenschein, W. M., Mattson, J., Basham, B., Sedgwick, J. D., McClanahan, T., Kastelein, R. A., and Cua, D. J. (2005). IL-23 drives a pathogenic T cell population that induces autoimmune inflammation. *J. Exp. Med.* **201,** 233–240.

Lertratanangkoon, K., and Horning, M. G. (1982). Metabolism of carbamazepine. *Drug Metab. Dispos.* **10,** 1–10.

Lotze, M. T., Zeh, H. J., Rubartelli, A., Sparvero, L. J., Amoscato, A. A., Washburn, N. R., Devera, M. E., Liang, X., Tör, M., and Billiar, T. (2007). The grateful dead: Damage-associated molecular pattern molecules and reduction/oxidation regulate immunity. *Immunol. Rev.* **220,** 60–81.

Lu, W., and Uetrecht, J. P. (2008). Peroxidase-mediated bioactivation of hydroxylated metabolites of carbamazepine and phenytoin. *Drug Metab. Dispos.* **36,** 1624–1636.

Mu, H. H., Hasebe, A., Van Schelt, A., and Cole, B. C. (2011). Novel interactions of a microbial superantigen with TLR2 and TLR4 differentially regulate IL-17 and Th17-associated cytokines. *Cell. Microbiol.* **13,** 374–387.

Novartis Pharma Co. (2011). *Interview Form (Product Information Booklet) of Tegretol®*, 9th ed. Novartis Pharma Co.,Tokyo, Japan.

Oo, Y. H., and Adams, D. H. (2009). The role of chemokines in the recruitment of lymphocytes to the liver. *J. Autoimmun.* **34,** 45–54.

Oscarson, M., Zanger, U. M., Rifki, O. F., Klein, K., Eichelbaum, M., and Meyer, U. A. (2006). Transcriptional profiling of genes induced in the livers of patients treated with carbamazepine. *Clin. Pharmacol. Ther.* **80,** 440–456.

Park, B. K., Kitteringham, N. R., Powell, H., and Pirmohamed, M. (2000). Advances in molecular toxicology-towards understanding idiosyncratic drug toxicity. *Toxicology* **153,** 39–60.

Pearce, R. E., Lu, W., Wang, Y., Uetrecht, J. P., Correia, M. A., and Leeder, J. S. (2008). Pathways of carbamazepine bioactivation in vitro. III. The role of human cytochrome P450 enzymes in the formation of 2,3-dihydroxycarbamazepine. *Drug Metab. Dispos.* **36,** 1637–1649.

Pearce, R. E., Vakkalagadda, G. R., and Leeder, J. S. (2002). Pathways of carbamazepine bioactivation *in vitro* I. Characterization of human cytochromes

P450 responsible for the formation of 2- and 3-hydroxylated metabolites. *Drug Metab. Dispos.* **30,** 1170–1179.

Pellinen, P., Honkakoski, P., Stenbäck, F., Niemitz, M., Alhava, E., Pelkonen, O., Lang, M. A., and Pasanen, M. (1994). Cocaine N-demethylation and the metabolism-related hepatotoxicity can be prevented by cytochrome P450 3A inhibitors. *Eur. J. Pharmacol.* **270,** 35–43.

Pirmohamed, M., Kitteringham, N. R., Breckenridge, A. M., and Park, B. K. (1992a). Detection of an autoantibody directed against human liver microsomal protein in a patient with carbamazepine hypersensitivity. *Br. J. Clin. Pharmacol.* **33,** 183–186.

Pirmohamed, M., Kitteringham, N. R., Guenthner, T. M., Breckenridge, A. M., and Park, B. K. (1992b). An investigation of the formation of cytotoxic, protein-reactive and stable metabolites from carbamazepine in vitro. *Biochem. Pharmacol.* **43,** 1675–1682.

Savov, J. D., Brass, D. M., Lawson, B. L., McElvania-Tekippe, E., Walker, J. K., and Schwartz, D. A. (2005). Toll-like receptor 4 antagonist (E5564) prevents the chronic airway response to inhaled lipopolysaccharide. *Am. J. Physiol. Lung Cell Mol. Physiol.* **289,** L329–L337.

Steinman, L. (2007). A brief history of T(H)17, the first major revision in the T(H)1/T(H)2 hypothesis of T cell-mediated tissue damage. *Nat. Med.* **13,** 139–145.

Sugawara, Y., Kubota, K., Ogura, T., Esumi, H., Inoue, K., Takayama, T., and Makuuchi, M. (1998). Protective effect of prostaglandin E1 against ischemia/reperfusion-induced liver injury: Results of a prospective, randomized study in cirrhotic patients undergoing subsegmentectomy. *J. Hepatol.* **29,** 969–976.

Talpain, E., Armstrong, R. A., Coleman, R. A., and Vardey, C. J. (1995). Characterization of the PGE receptor subtype mediating inhibition of superoxide production in human neutrophils. *Br. J. Pharmacol.* **114,** 1459–1465.

Wang, H., Yang, H., and Tracey, K. J. (2004). Extracellular role of HMGB1 in inflammation and sepsis. *J. Intern. Med.* **255,** 320–331.

Yao, D., and Brownlee, M. (2010). Hyperglycemia-induced reactive oxygen species increase expression of the receptor for advanced glycation end products (RAGE) and RAGE ligands. *Diabetes* **59,** 249–255.

The Journal of Toxicological Sciences (J. Toxicol. Sci.)
Vol.37, No.5, 931-942, 2012

Original Article

Hepatoprotective effect of tamoxifen on steatosis and non-alcoholic steatohepatitis in mouse models

Taishi Miyashita[1], Yasuyuki Toyoda[1], Koichi Tsuneyama[2], Tatsuki Fukami[1], Miki Nakajima[1] and Tsuyoshi Yokoi[1]

[1]Drug Metabolism and Toxicology, Faculty of Pharmaceutical Sciences, Kanazawa University, Kakuma-machi, Kanazawa 920-1192, Japan
[2]Department of Diagnostic Pathology, Graduate School of Medicine and Pharmaceutical Science for Research, University of Toyama, Sugitani 930-0194, Toyama, Japan

(Received June 9, 2012; Accepted July 3, 2012)

ABSTRACT — Non-alcoholic fatty liver disease (NAFLD) is characterized by hepatic lipid accumulation that starts with steatosis and progresses to non-alcoholic steatohepatitis (NASH). Recently, the number of patients with such liver diseases has increased, but the understanding of the fundamental mechanisms and appropriate therapies are lacking. Tamoxifen (TAM) is a selective estrogen receptor modulator. We previously reported that TAM plays a protective role against drug-induced and chemical-induced acute liver injuries. However, the effects of TAM on chronic liver injury, including steatosis and NASH, remain to be addressed. We first found that the administration of TAM to mouse models of steatosis and NASH significantly decreased the plasma ALT and AST levels. The administration of TAM decreased the accumulated fat and inflammation in the livers in both mouse models. In addition, we observed decreased hepatic mRNA levels of triglyceride synthesis, acyl-CoA: diacylglycerol acyltransferase 2 (DGAT2), proinflammatory cytokines, tumor necrosis factor (TNF) α, and chemokines, monocyte chemoattractant protein (MCP) -1. TAM increased the extracellular signal-regulated kinase (ERK) phosphorylation, which is related to the proliferation and regeneration of liver and to decreased DGAT2 gene expression. Furthermore, a decrease in eukaryotic translational initiation factor (eIF2α), which is involved in apoptosis, was observed in both models. These findings suggest that TAM treatment exerts a hepatoprotective effect against steatosis and NASH, presumably via up-regulation of the ERK pathways and attenuation of eIF2α activation. These pathways represent a potential therapeutic target for steatosis and NASH in drug development.

Key words: Steatosis, NASH, Tamoxifen, ERK

INTRODUCTION

Non-alcoholic fatty liver disease (NAFLD) is now recognized as an important health concern (Angulo, 2002). NAFLD is characterized by hepatic lipid accumulation that starts with steatosis and progresses to non-alcoholic steatohepatitis (NASH) with progressive fibrosis. The histopathological features of NASH include evidence of steatosis, liver cell injury, a mixed inflammatory lobular infiltrate, and variable degrees of fibrosis (Ludwig *et al.*, 1980). The pathogenic mechanism of steatosis is related to fatty acid metabolism in the liver (Donnelly *et al.*, 2005). In the pathogenesis of NASH, a "two hit" theory has been proposed. Fat accumulation in the liver is the "first hit". Fat makes the liver vulnerable to endotoxins and ischemic reperfusion damage, impairs liver regeneration (Uesugi *et al.*, 2001) and causes hepatic insulin resistance (Kim *et al.*, 2001). Acyl-CoA: diacylglycerol acyltransferase 2 (DGAT2) is the final step and rate limiting reaction in triglyceride synthesis (Choi *et al.*, 2007; Yu *et al.*, 2005; Wang *et al.*, 2010). Reactive oxygen species (ROS) together with tumor necrosis factor (TNF) α and monocyte chemoattractant protein (MCP) -1 represent the "second hit" (Jou *et al.*, 2008). Fatty acids can deliver both hits. In general, chronic liver injury can be improved by diet and exercise, but fundamental medications for such liver injury have not been established.

Estrogen binds estrogen receptor and contributes to

Correspondence: Tsuyoshi Yokoi (E-mail: tyokoi@p.kanazawa-u.ac.jp)

downstream biological reactions. Estrogen receptor exists as two subtypes, estrogen receptor α and β. In the liver, estrogen receptor α is the principally expressed form, and estrogen receptor β is expressed at only low levels (Kuiper *et al.*, 1997). Estrogen-treated mice are reportedly protected from the injurious effects of hepatic ischemia and reperfusion, and estrogen protected mice from diethylnitrosamine-induced hepatocarcinogenesis (Harada *et al.*, 2004; Naugler *et al.*, 2007). These results suggest that estrogen plays a protective role in the pathology of hepatotoxicity. However, there has been little information concerning the potential functional role of estrogen after the onset of hepatotoxicity in steatosis and NASH.

Tamoxifen (TAM) is a selective estrogen receptor modulator (SERM) that can act as either an estrogen agonist or an estrogen antagonist, depending on the tissue (Dhingra, 1999). TAM acts as an antagonist in the mammary gland, but acts as an agonist in the uterus, bone tissue, and liver (Obsorne and Fuqua, 1994; Mitlak and Cohen, 1997; Cosman and Lindsay, 1999). We previously reported that TAM plays a protective role against drug-induced and chemical-induced acute liver injuries (Yoshikawa *et al.*, 2012). However, the effects of TAM on chronic liver injury, including steatosis and NASH, remain to be addressed.

In this study, we investigated whether TAM plays a protective role in mouse models of steatosis and NASH. Furthermore, we elucidated the factors that attenuate liver injury by administration of TAM.

MATERIALS AND METHODS

Materials

TAM was obtained from Wako Pure Chemical Industries (Osaka, Japan). Primers were commercially synthesized at Hokkaido System Sciences (Hokkaido, Japan). Monoclonal antibodies against anti-Thr202/Tyr204-phosphorylated extracellular signal-regulated kinase (ERK) 1/2, anti-Thr180/Tyr182-phosphorylated p38 mitogen-activated protein kinase (MAPK), and anti-Thr183/Tyr185 phosphorylated c-Jun N-terminal kinase (JNK) 1/2 were purchased from Cell Signaling Technology (Beverly, MA, USA). Monoclonal antibodies against ERK1/2 and JNK1/2 and the polyclonal antibodies against p38 MAPK, eukaryotic initiation factor 2 (eIF2α) and anti-Ser51-phosphorylated eIF2α were also obtained from Cell Signaling Technology. IRDye680-labeled goat anti-rabbit or anti-mouse secondary anti body and Odyssey Blocking Buffer were from Li-COR Biosciences (Lincoln, NE, USA). All other reagents were of the highest grade commercially available.

Animal treatments

Female ICR (7 weeks old, 27-29 g) were obtained from SLC Japan (Shizuoka, Japan). Animals were housed in a controlled environment (temperature 25 ± 1°C, humidity 50 ± 10%, and 12-hr light/12-hr dark cycle) in the institutional animal facility with access to food and water *ad libitum*. Mice were fed a normal diet, high-fat-diet (HFD) or methionine and choline deficient diet (MCDD) for 10 weeks. After 9 weeks of diet, the mice were divided into 2 groups. TAM (1 mg/kg) dissolved in saline was intraperitoneally administered for 5 consecutive days. We previously reported that administration of TAM for 5 days demonstrated hepatoprotective effects against chemical-induced acute liver injuries (Yoshikawa *et al.*, 2012). Twelve hours after the final administration of TAM, the mice were sacrificed. The liver was fixed in buffered neutral 10% formalin and used for immunohistochemical staining. The degree of liver injury was assessed by hematoxylin-eosin (H&E) staining and the plasma aspartate aminotransferase (AST) and alanine aminotransferase (ALT) levels were determined using Fuji DRI-CHEM 4000V (Fuji Film Med. Co., Tokyo, Japan). Animal maintenance and treatment were conducted in accordance with the National Institutes of Health Guide for Animal Welfare of Japan, as approved by the Institutional Animal Care and Use Committee of Kanazawa University, Japan.

GSH level

Livers (50 mg) were homogenized with ice-cold 5% sulfosalicylic acid and centrifuged at 8,000 × g at 4°C for 10 min. The GSH concentration in the supernatant was measured as described previously (Tietze, 1969).

Lipid peroxidation measurement

Lipid peroxidation was measured using Aldetect Lipid Peroxidation Assay kit (Enzo Life Sciences, NY, USA). In brief, for each reaction, 10 μl of probucol and 640 μl of diluted R1 reagent (1:3 of methanol: N-methyl-2-phenylindole) were added to 10 mg of liver homogenate and mixed with 150 μl of 12 M HCl. Each reaction was incubated at 45°C for 60 min and centrifuged at 10,000 × g for 10 min. The supernatant was used to measure malondialdehyde (MDA) formation at 586 nm.

Real-time reverse transcription (RT)-PCR

RNA from mouse liver was isolated using RNAiso (Takara Bio, Shiga, Japan) according to the manufacturer's instructions. Carnitine palmitoyl transferase-1 (CPT-1), acyl-CoA: diacylglycerol acyltransferase 2 (DGAT2), fatty acid synthase (FASN), monocyte chemoattractant protein (MCP) -1, sterol regulatory element-binding protein-1

(SREBP-1), tumor necrosis factor (TNF) α, and glyceraldehyde-3-phosphate dehydrogenase (Gapdh) were quantified by real-time RT-PCR. The primer sequences used in this study are shown in Table 1. The reverse transcription process, total RNA (4 μg) and 150 ng random hexamer were mixed and incubated at 70°C for 10 min. The RNA solution was added to a reaction mixture containing 100 units of ReverTra Ace, reaction buffer and 0.5 mM dNTPs in a final volume of 40 μl. The reaction mixture was incubated at 30°C for 10 min, 42°C for 1 hr and heated at 98°C for 10 min to inactivate the enzyme. The real-time RT-PCR was performed using the Mx3000P real-time PCR system (Stratagene, La Jolla, CA, USA). The PCR mixture contained 1 μl of template cDNA, SYBR Premix Ex Taq solution and 8 pmol forward and reverse primers. Amplified products were monitored directly by measurring the increase of the dye intensity of the SYBR Green I (Molecular Probes, Eugene, OR, USA) that binds to the double-strand DNA amplified by PCR.

Immunoblot analysis

SDS-polyacrylamide gel electrophoresis and immunoblot analysis were performed. Mouse liver homogenates (50 μg) were separated on 10% polyacrylamide gels and electrotransferred onto polyvinylidene difluoride membranes, Immobilon-P (Millipore Corporation, Billerica, MA, USA). The membranes were probed with the monoclonal antibodies against anti-Thr202/Tyr204-phosphorylated ERK1/2, anti-Thr180/Tyr182-phosphorylated p38 MAPK, and anti-Thr183/Tyr185-phosphorylated JNK1/2, rabbit anti-human GAPDH antibodies, and mouse anti-KDEL antibodies and incubated with IRDye680-labeled goat anti-rabbit or anti-mouse IgG secondary antibody diluted with PBST. The Odyssey Infrared Imaging system (Li-COR Biosciences, Lincoln, NE, USA) was used for the detection. The relative expression levels were quantified using ImageQuant TL Image Analysis software (GE Healthcare, Little Chalfont, Buckinghamshire, UK).

Statistical analysis

Data are presented as the mean ± S.D. Comparisons of 2 groups were made with an unpaired, two-tailed Student's t-test. Comparisons of multiple groups were made with ANOVA followed by Dunnett or Turkey test. A value of $P < 0.05$ was considered statistically significant.

RESULTS

Effects of TAM on hepatic injury in steatosis or NASH model mice

Mice were fed HFD or MCDD for 10 weeks. The plasma ALT and AST levels in steatosis and NASH mice models were significantly increased compared with CTL mice. Treatment with TAM (1 mg/kg, *i.p.*, 5 days) resulted in significantly decreased ALT and AST levels in both mouse models compared with TAM-unadministered CTL mice (Fig. 1A). Hepatocytes in the HFD-fed mice exhibited different sizes of lipid droplets and inflammation. The

Table 1. Sequences of primers used for real-time RT-PCR analysis in this study

Gene	Primer	Sequence
CPT-1	FP	5'-GCA TAC CAA AGT GGA CCC CT-3'
	RP	5'-TGC TCT GCA AAC ATC CAG CC-3'
DGAT2	FP	5'-CAT GAA GAC CCT CAT CGC CG-3'
	RP	5'-GTG ACA GAG AAG ATG TCT TGG-3'
FASN	FP	5'-GCT CCT CGC TTG TCG TCT G-3'
	RP	5'-GAT CCT TCA GCT TTC CAG AC-3'
MCP-1	FP	5'-TGT CAT GCT TCT GGG CCT G-3'
	RP	5'-CCT CTC TCT TGA GCT TGG TG-3'
SREBP-1	FP	5'-GAA CAG ACA CTG GCC GAG ATG-3'
	RP	5'-AGG AGG CCA GAG AAG CAGAAG-3'
TNF-α	FP	5'-TGT CTC AGC CTC TTC TCA TTC C-3'
	RP	5'-TGA GGG TCT GGG CCA TAG AAC-3'
Gapdh	FP	5'-AAA TGG GGT GAG GCC GGT-3'
	RP	5'-ATT GCT GAC AAT CTT GAG TGA-3'

FP, forward primer; RP, reverse primer.

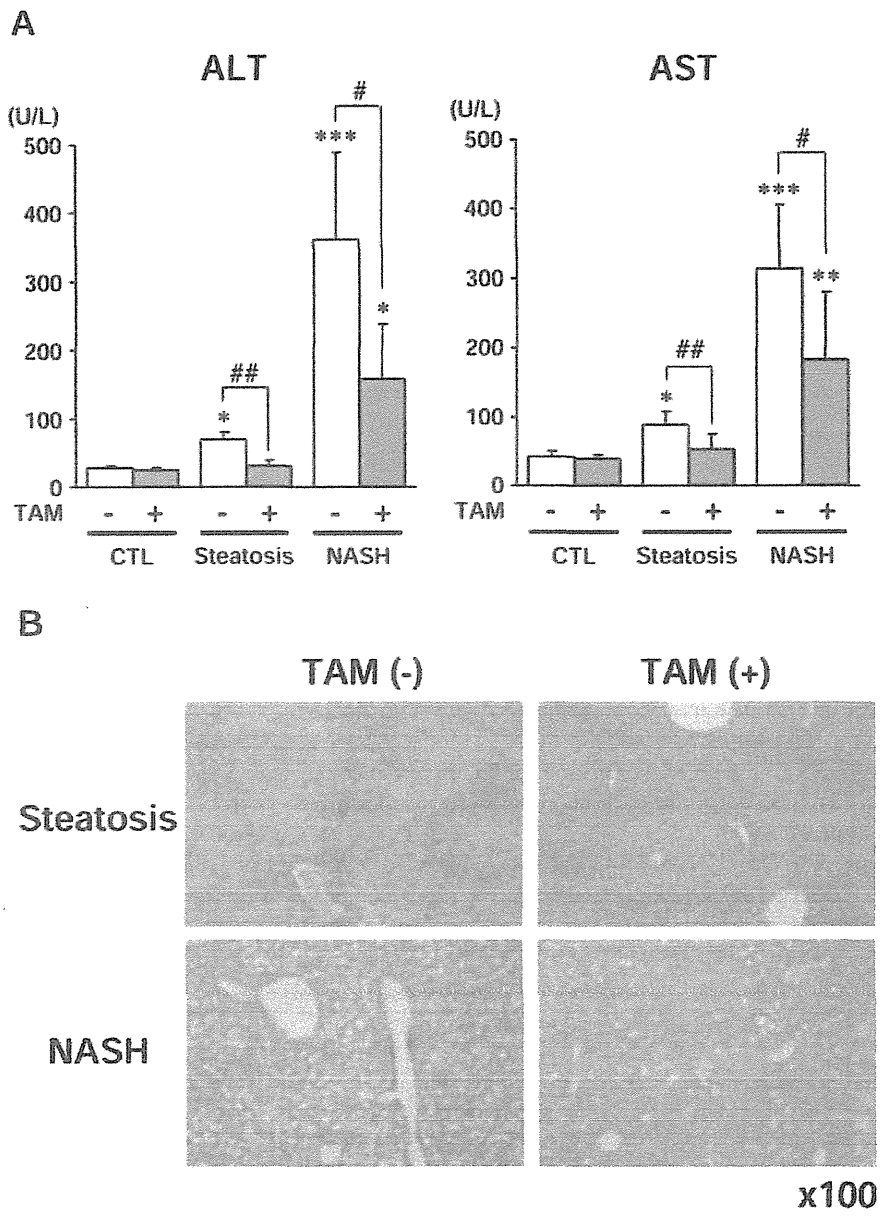

Fig. 1. Effects of tamoxifen (TAM) on hepatic injury in steatosis or non-alcoholic steatohepatitis (NASH) model mice. Mice were administered TAM for 5 days (1 mg/kg, *i.p.*). Plasma alanine aminotransferase (ALT) and aspartate aminotransferase (AST) levels were measured 12 hr after the last administration of TAM (A). Hematoxylin-eosin staining was performed in excised liver sections of steatosis or NASH model mice (B). Data are shown as the mean ± S.D. of results from 4-5 mice. Differences from the control (CTL) mice were considered significant at $^{*}p < 0.05$, $^{**}p < 0.01$ and $^{***}p < 0.001$, and differences from the TAM-unadministered model mice were considered significant at $^{\#}p < 0.05$ and $^{\#\#}p < 0.01$.

livers of mice fed MCDD exhibited macrovesicular steatosis, ballooning degeneration of hepatocytes, and lobular inflammation (Fig. 1B). No effect of TAM on CTL mice was observed (data not shown). Thus, feeding with HFD and MCDD for 10 weeks induced steatosis and NASH in mice. TAM-administration decreased the accumulated fat and inflammation in the livers of both mouse models. The attenuation of hepatic steatosis resulted in decreased

hepatic inflammation in TAM-administered mice.

Effects of TAM on oxidative stress in the livers of steatosis or NASH model mice

Glutathione (GSH) detoxifies ROS produced in the mitochondrial electron transport chain (Okabe *et al.*, 1994). The ratios of GSH/ glutathione disulfide (GSSG) and MDA are often used as markers of cellular toxicity and oxidative stress and appear to increase during NAFLD progression (Caballero *et al.*, 2010). To investigate whether the oxidative stress was modulated by TAM, GSH/GSSG ratio and MDA levels in the liver were measured (Fig. 2). The ratios of GSH/GSSG in the steatosis and NASH model mice were significantly decreased compared with CTL mice, but TAM treatment produced no effect on the ratio of GSH/GSSG in the livers of the mice. MDA levels were significantly increased in steatosis and NASH model mice compared with CTL mice, but TAM had no effect on MDA (Fig. 2). These results suggest that administration of TAM is not likely to affect oxidative stress.

Effects of TAM on hepatic mRNA expression of SREBP-1, FASN, CPT-1 and DGAT2 in steatosis or NASH model mice

The expression of genes involved in fatty acid metabolism in the liver was investigated. The expression of SREBP-1, a transcription factor that activates genes involved in lipogenesis, was unchanged in the steatosis and NASH model mice. The administration of TAM did not affect the expression of SREBP-1 in either mouse models. The expressions of FASN, an enzyme involved in fatty acid synthesis, was significantly decreased in the steatosis and NASH model mice compared with the CTL mice. In CTL mice, the expression of FASN was significantly increased by TAM, but TAM did not alter FASN expression in the steatosis and NASH model mice compared with the TAM-unadministered mice. In the steatosis model mice, the expression of CPT-1, a rate-limiting regulator of mitochondrial β-oxidation and mitochondrial fatty acid import, was significantly increased in the steatosis model mice compared with the CTL mice. The administration of TAM significantly decreased CPT-1 compared with the TAM-unadministered steatosis model mice. In the NASH model mice, the expression of CPT-1 was significantly decreased compared with the CTL mice. However, the administration of TAM did not affect the expression of CPT-1 compared with TAM-unadministered NASH model mice (Fig. 3). The expression of DGAT2, a rate limiting enzyme in triglyceride synthesis, was significantly decreased in CTL and both mouse models by TAM. These results suggest that TAM may be involved in decreasing the hepatic fat accumulation in both mouse models, and may inhibit β-oxidation of fatty acid in the steatosis model mice.

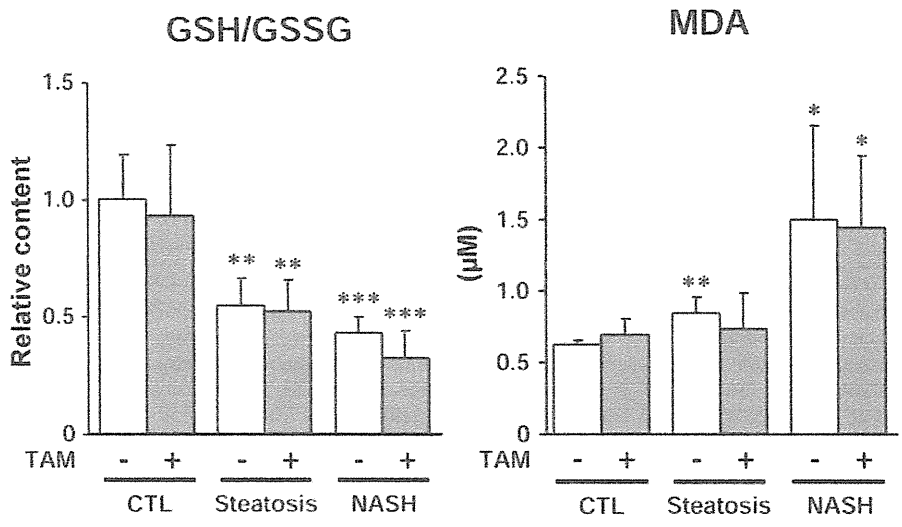

Fig. 2. Effects of tamoxifen (TAM) on the ratios of glutathione (GSH)/ glutathione disulfide (GSSG) and on oxidative stress in steatosis or non-alcoholic steatohepatitis (NASH) model mice. The ratios of GSH/GSSG and the malondialdehyde (MDA) levels were measured 12 hr after the last administration of TAM. Data are shown as the mean ± S.D. of results from 4-5 mice. Differences compared to the control (CTL) mice were considered significant at $*p < 0.05$, $**p < 0.01$ and $***p < 0.001$.

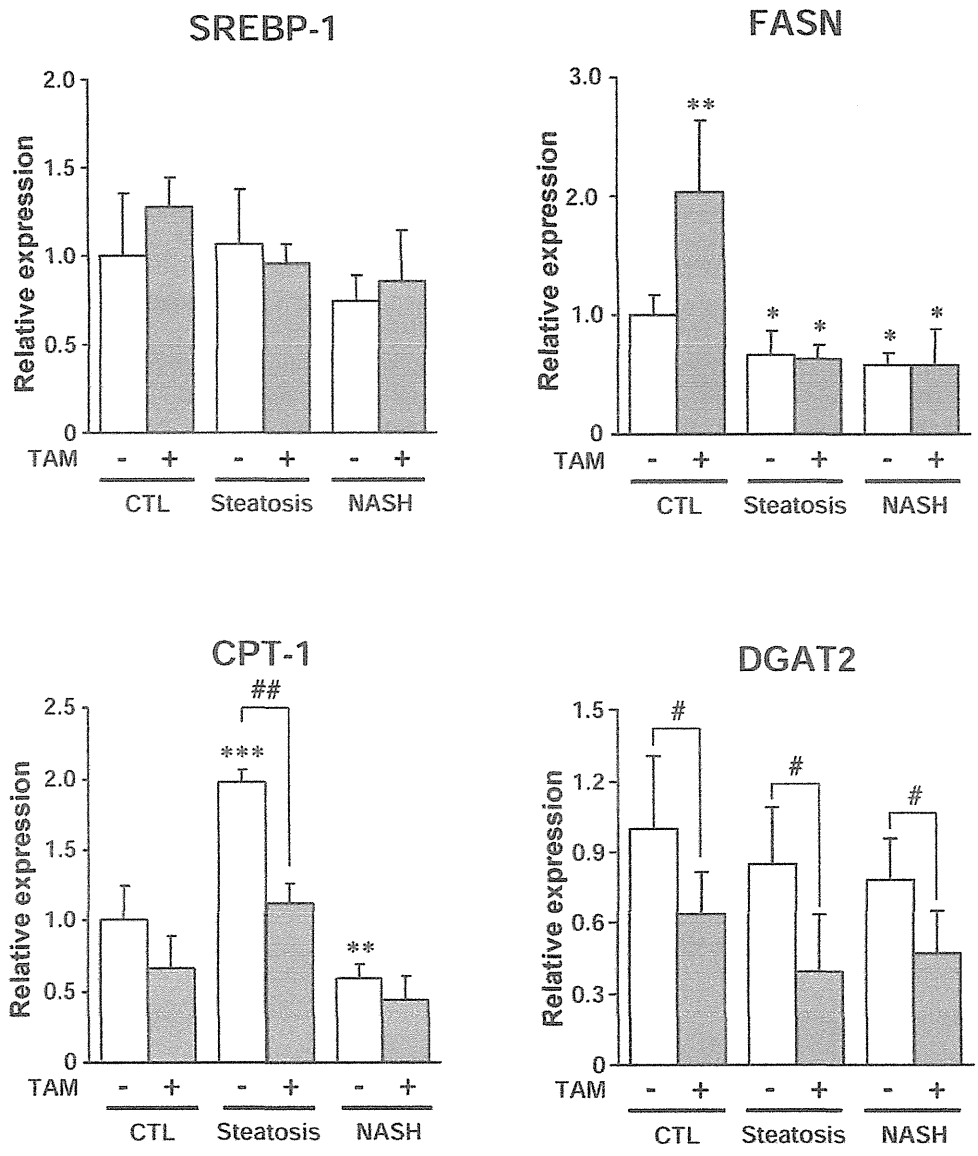

Fig. 3. Effects of tamoxifen (TAM) on hepatic mRNA expression of sterol regulatory element-binding protein-1 (SREBP-1), fatty acid synthase (FASN), acyl-CoA: diacylglycerol acyltransferase 2 (DGAT2) and carnitine palmonitoyl transferase-1 (CPT-1) in steatosis or non-alcoholic steatohepatitis (NASH) model mice. Mice were administered TAM for 5 days (1 mg/kg, *i.p.*). The expression of hepatic mRNA was normalized to glyceraldehyde-3-phosphate dehydrogenase (Gapdh) in each mouse. Data are shown as the mean ± S.D. of results from 4-5 mice. Differences from the control (CTL) mice were considered significant at $^{*}p < 0.05$, $^{**}p < 0.01$ and $^{***}p < 0.001$, and differences from the TAM-unadministered model mice were considered significant at $^{\#\#}p < 0.01$.

Effects of TAM on hepatic mRNA expression of TNFα and MCP-1 in steatosis or NASH model mice

The proinflammatory cytokine TNFα and the chemokine MCP-1 are known to play an important role in the development and progression of hepatic inflammation (Anstee and Goldin, 2006). To investigate whether TAM affected the production of inflammatory cytokines and chemokines, hepatic mRNA of TNFα and MCP-1 was measured. In our previous study (Higuchi *et al.*,